Triterpenoids from the Stem Bark of *Aglaia cucullata* (Meliaceae) and Their Cytotoxic Activity against A549 Lung Cancer Cell Line

Desi Harneti[1*], Iqbal Wahyu Mustaqim[1], Darwati Darwati[1], Al Arofatus Naini[1], Purnama Purnama[1], Erina Hilmayanti[1], Tri Mayanti[1], Nurlelasari Nurlelasari[1], Shabarni Gaffar[1], Rani Maharani[1], Kindi Farabi[1], Unang Supratman[1,2], Sofa Fajriah[3], Mohamad Nurul Azmi[4], and Yoshihito Shiono[5]

[1]*Department of Chemistry, Faculty of Mathematics and Natural Sciences, Universitas Padjadjaran, Jl. Raya Bandung-Sumedang Km. 21, Jatinangor, Sumedang 45363, Indonesia*

[2]*Central Laboratory, Universitas Padjadjaran, Jl. Raya Bandung-Sumedang Km. 21, Jatinangor, Sumedang 45363, Indonesia*

[3]*Research Center for Pharmaceutical Ingredients and Traditional Medicine, National Research and Innovation Agency (BRIN), Komplek Cibinong Science Center – BRIN, Jl. Raya Bogor Km. 46, Cibinong 16911, Indonesia*

[4]*School of Chemical Sciences, Universiti Sains Malaysia, 11800 Minden, Malaysia*

[5]*Department of Food, Life, and Environmental Science, Faculty of Agriculture, Yamagata University, Tsuruoka, Yamagata 997-8555, Japan*

* ***Corresponding author:***

email: desi.harneti@unpad.ac.id

Received: October 31, 2022
Accepted: March 2, 2023

DOI: 10.22146/ijc.78748

Abstract: *The* Aglaia *species, which contains triterpenoids, is the most numerous in the Meliaceae family. The* A. cucullata *species, of which there are only a few known examples, has received scant research attention. This investigation aims to identify triterpenoids in an* n*-hexane preparation of* A. cucullata *stem bark and evaluate their effects against the A549 lung cancer cell line. Five dammarane-type triterpenoids were isolated from the* A. cucullata *trunk bark, which is (1) (20S)-20-hydroxydammar-24-en-3-one, (2) cabraleone, (3) cabralealactone, (4) eichlerianic acid, and (5) (+)-fouquierol. Their chemical structures were determined using infrared, high-resolution mass spectrometry, and nuclear magnetic resonance, as well as through data comparison of the reported compounds. Compound* ***1*** *was priorly separated from the* Aglaia *genus, compounds* ***2–4*** *were first isolated from the* A. cucullata *species, and compound* ***5*** *has been reportedly isolated from the Meliaceae family and the* Aglaia *genus. All substances were tested for their lethal potential against the A549 lung cancer cell type. A* seco *structure in the A ring of dammarane-type triterpenoid might play an important part in the lethal activity of component 4, which showed the greatest activity with an* IC_{50} *value of 32.17 μM against the A549 lung cancer cell line.*

Keywords: Aglaia cucullate*; cytotoxic activity; lung cancer cell (A549); Meliaceae triterpenoids*

■ INTRODUCTION

Terpenoids, including the crucial triterpenoids, are produced via the acetate/mevalonate route in the cytoplasm and endoplasmic membrane [1-2]. Their carbon structure is made of six isoprene units. Eukaryotic species have been found to contain more than 20,000 triterpenoids [1] and around 200 distinct structures. Higher plants typically contain triterpenoids, which serve as a first line of defense against microbes, parasites, and predators [3-4]. Based on their molecular structure, triterpenoids are categorized as either acyclic [5-6], monocyclic [6-7], bicyclic [8-9], tetracyclic [10-11], pentacyclic [12], or hexacylic [5-6]. There are many potential health benefits associated with triterpenoids, including anti-inflammatory [13-14], antioxidant [15], antibacterial [16-17], antiviral [18-19], antifungal [20-

21], hepatoprotective [20-21], anti-disease Alzheimer's [21], immunomodulatory [22-23], cytotoxic [24], and anticancer [25-26]. *Cedrela* [25], *Turraea* [26], *Entandrophragma* [27], *Azadirachta* [28], *Guarea* [29], *Lansium* [30], *Chisocheton* [31], *Melia* [32], *Dysoxylum* [33], *Toona* [34], and *Aglaia* [35] are all examples of taxa in the Meliaceae family that contain triterpenoids.

A. cucullata (Roxb.) Pellegr, also called Pacific maple, is a mangrove plant that belongs to the *Aglaia* genus [36-37]. *A. cucullata* is a tall tree that grows in coastal forests in tropical regions such as India, Bangladesh, Myanmar, Thailand, Malaysia, and Indonesia [38-39]. This species is widely spread in several regions in Indonesia, including in northern Sumatra and Kalimantan, southern Sulawesi coast, Halmahera, Ambon, Aru, and Irian Jaya [37]. Moreover, the plant's timber is utilized for boat construction, house supports, and fuel wood [38], while the leaves and fruits are for treating diarrhea, dysentery, skin infections, and cardiac diseases by Thai people [40], and as anti-inflammation and rheumatism by Burma people [41]. Flavaglines with cytotoxic activity towards oral human KB, breast cancer cells in human BC, and small cell lung NCI-H187 [40], bisamides [42], kaurane and labdane diterpenoids, and cycloartane triterpenoid with TRAIL resistance-overcoming activity [38] have been isolated through chemical analysis of this species. In our ongoing efforts to search for triterpenoids from the Indonesian *Aglaia* plants, we have further investigated the stem bark of *A. cucullata.* As a result, five triterpenoids (**1**–**5**) were successfully isolated and elucidated. Compound **1** was reported first time in the *Aglaia* genus, compounds **2**–**4** were found in *A. cucullata* for the first time, while compound **5** was discovered for the first time in *Meliaceae* family and *Aglaia* genus. All isolated compounds were assayed against A549 lung cancer cell lines. The detail of isolation, structure elucidation, and cytotoxic activity are described in this article.

■ EXPERIMENTAL SECTION

Materials

The stem bark of *A. cucullata* was obtained from the Manggar River, Balikpapan, East Kalimantan, in December 2020. The plant was examined at the Herbarium Wanariset, Balikpapan (collection No. FF7.20), and stored at the Faculty of Forestry, Universitas Mulawarman.

For extraction, fractionation, isolation, and purification, the following pro analyst and technical grade solvents are utilized: chloroform p.a. (Merck), acetone, methanol (MeOH), ethanol, ethyl acetate (EtOAc), *n*-butanol, *n*-hexane (Sigma-Aldrich), A549 cells were obtained from American Type Culture Collection (ATCC® CCL-185TM, Virginia, USA). Roswell Memorial Park Medium (RPMI) 1640 (Cat. No.11530586, Gibco, USA), 10% Fetal Bovine Serum (FBS, Cat. No.10082147, Gibco), and 1% Penicillin-Streptomycin were used to cultivate the cells (Cat. No. 15140112, Gibco). The cells were incubated at 37 °C in an incubator containing 5% CO_2 (Cat. No. 8000DH, Thermo Fisher Scientific, USA).

Instrumentation

A PerkinElmer Spectrum 100 FTIR spectrometer (PerkinElmer, USA) was utilized to characterize the KBr plate's IR spectrum. Using a Waters Xevo QTOF mass spectrometer (Waters, USA), mass spectra were acquired. Tetramethyl silane (TMS) was used as an internal standard, and NMR spectra were obtained using a Bruker Av-500 spectrometer (Bruker, Germany) at 500 MHz for ^{1}H-NMR and 125 MHz for ^{13}C-NMR. The column chromatography on ODS RF-18 and silica G_{60} was conducted using thin layer chromatography (TLC) on a silica G_{60} GF_{254} (Merck, 0.25 mm) column and a variety of solvent systems (Merck, 70–230 and 230–400 mesh). Spots were discovered using 10% H_2SO_4 in ethanol, which was heated and then examined under UV light at 254 and 365 nm.

Procedure

Extraction and isolation

The pulverized stem bark of *A. cucullata* was macerated in ethanol for 7 d (40 L). Using a rotary vacuum evaporator at 40 °C, the ethanol solvent was evaporated to produce a concentrated ethanol extract residue (523 g). The crude ethanol extract was suspended in a 4:1 ethanol:water mixture and partitioned with each substance to obtain the crude

extracts of *n*-hexane (128 g), EtOAc (35.7 g), and *n*-butanol (13.1 g). The *n*-hexane crude extract was separated by vacuum-liquid chromatography (VLC) on silica G_{60} eluting with *n*-hexane:EtOAc:MeOH (100:0–0:100, 10% v/v) to produce seven fractions (A-G). Fraction C (16.2 g) was further separated by VLC on silica G_{60} and eluted with *n*-hexane:EtOAc (100:0–50:50, 10% v/v) to yield four subfractions (C1-C4). Subfraction C2 (1.28 g) was subjected to column chromatography (CC) on silica gel (230–400 mesh) eluted with *n*-hexane:EtOAc (100:0–80:20, 1% v/v) to produce four subfractions (C2A-C2D). Subfraction C2B (160.8 mg) was further purified with CC over silica gel (230–400 mesh) eluted with *n*-hexane:EtOAc (8:2) to give compound **1** (13.2 mg). Subfraction C2C (562.8 mg) was further separated with CC over silica gel (230–400 mesh) eluted with *n*-hexane:EtOAc (90:10, v/v) to yield five subfractions (C2C1-C2C5). Subfraction C2C2 (243.8 mg) was purified by CC over silica gel (230–400 mesh) eluted with *n*-hexane: EtOAc (85:15, v/v) to yield compound **2** (113.3 mg). In addition, subfraction C4 (12.7 g) was separated using CC on silica gel (70–230 mesh) and eluted with *n*-hexane: EtOAc (100:0–30:70, 2% v/v) to generate ten subfractions (C4A-C4J). Subfraction C4E (2.4 g), which was separated by CC over silica gel (230–400 mesh) and eluted with *n*-hexane: EtOAc (80:20, v/v) to give four subfractions (C4E1-C4E4). Subfraction C4E2 (276.3 mg) was separated using CC silica gel (230–400 mesh) and an isocratic mixture of *n*-hexane, chloroform, and EtOAc (50:40:10, v/v) to give compound **3** (15.5 mg). Subfraction C4E2D (83 mg) was purified by reverse-phase CC on ODS eluted with MeOH: water (80:20, v/v) to give compound **4** (5.3 mg). Subfraction C4E2E (26.7 mg) was purified by CC over silica gel (230–400 mesh) *via* an isocratic mixture of *n*-hexane:chloroform:EtOAc to yield **5** (10.2 mg).

(20*S*)-20-hydroxydammar-24-en-3-one (1). White crystal, m.p. 166–168 °C, IR ν_{max} (cm^{-1}): 3448, 2955, 1704, 1378, 1018. ^{1}H-NMR ($CDCl_3$, 500 MHz) and ^{13}C-NMR spectral data ($CDCl_3$, 125 MHz) are shown in Table 1. HR-TOFMS *m/z* found at 443.3817 $[M+H]^+$ (calculated for $C_{30}H_{51}O_2$, *m/z* = 443.3811).

Table 1. The summary result of NMR signal of (20*S*)-20-hydroxydammar-24-en-3-one (**1**) in $CDCl_3$ (δ in ppm, 500 MHz for ^{1}H and 125 MHz ^{13}C-NMR)

Position	^{13}C-NMR	^{1}H-NMR (ΣH, mult., *J*)	COSY	HMQC	HMBC
1	39.90	1.86 (2H, m)	H2	C1	-
2	34.10	2.37-2.42 (2H, m)	H1	C2	-
3	218.00	-	-	-	-
4	47.40	-	-	-	-
5	55.40	1.32 (1H, m)	H6	C5	-
6	19.70	1.49 (1H, dd, 6.5, 2.4), 1.40 (1H, d, 6.5)	H5/H7	C6	-
7	34.60	1.50 (1H, dd, 7.0, 2.5), 1.26 (1H, d, 7.0)	H6	C7	-
8	40.30	-	-	-	-
9	50.00	1.36 (1H, dd, 9.2, 2.7)	-	C9	-
10	36.80	-	-	-	-
11	22.00	1.45 (1H, dd, 8.5, 2.5), 1.25 (1H, d, 8.5)	H12	C11	-
12	27.50	1.79 (1H, d, 7.9), 1.23 (1H, dd, 7.9, 1.4)	H11/H13	C12	-
13	42.40	1.60 (1H, m)	H12	C13	-
14	50.30	-	-	-	-
15	31.20	1.40 (1H, ddd, 8.2, 6.6, 2.0), 1.03 (1H, dd, 6.6, 2.0)	H16	C15	-
16	24.80	1.69 (1H, dd, 7.0, 4.2), 1.44 (1H, d, 7.0)	H15/H17	C16	-
17	49.80	1.68 (1H, ddd, 9.1, 5.6, 2.1)	H16	C17	-
18	15.20	0.93 (3H, s)	-	C18	C7, C8, C9
19	16.00	0.88 (3H, s)	-	C19	C1, C5, C9, C10
20	75.40	-	-	-	-

Position	^{13}C-NMR	^{1}H-NMR (ΣH, mult., *J*)	COSY	HMQC	HMBC
21	25.50	1.08 (3H, s)	-	C21	C17, C20, C22
22	40.50	1.42 (2H, m)	H23	C22	C24
23	22.60	1.99 (2H, m)	H22/H24	C23	-
24	124.70	5.05 (1H, t, 6.1)	H23	C24	-
25	131.60	-	-	-	-
26	25.70	1.62 (3H, s)	-	C26	C24, C25
27	17.70	1.56 (3H, s)	-	C27	C24, C25
28	26.70	1.01 (3H, s	-	C28	C3, C4, C5
29	21.00	0.97 (3H, s)	-	C29	C3, C4, C5
30	16.40	0.82 (3H, s)	-	C30	C8, C13, C14, C15

Table 2. The summary result of the NMR signal of cabraleone (**2**) in $CDCl_3$ (δ in ppm, 500 MHz for ^{1}H and 125 MHz ^{13}C-NMR)

Position	^{13}C-NMR	^{1}H-NMR (ΣH, mult., *J*)	COSY	HMQC	HMBC
1	39.90	1.88 (1H, dd, 7.8, 2.4), 1.41 (1H, d, 7.8)	H2	C1	-
2	34.10	2.41 (2H, ddd, 6.5, 3.2, 1.6)	H1	C2	-
3	218.00	-	-	-	-
4	47.40	-	-	-	-
5	55.30	1.33 (1H, m)	H6	C5	-
6	19.70	1.50 (1H, dd, 8.2, 4.2), 1.41 (1H, d, 8.2)	H5/H7	C6	-
7	34.60	1.52 (1H, d, 6.5), 1.26 (1H, dd, 6.5, 2.1)	H6	C7	-
8	40.30	-	-	-	-
9	50.20	1.38 (1H, m)	-	C9	-
10	36.90	-	-	-	-
11	22.30	1.47 (1H, m), 1.21 (1H, m)	H12	C11	-
12	27.00	0.99 (2H, m)	H11/H13	C12	-
13	43.00	1.63 (1H, m)	H12	C13	-
14	50.00	-	-	-	-
15	31.40	1.43 (1H, m), 1.04 (1H, m)	H16	C15	-
16	25.80	1.74 (2H, m)	H15/H17	C16	-
17	49.80	1.82 (1H, m)	H16	C17	-
18	15.20	0.94 (3H, s)	-	C18	C7, C8, C9
19	16.10	0.88 (3H, s)	-	C19	C1, C5, C9, C10
20	86.50	-	-	-	-
21	27.10	1.09 (3H, s)	-	C21	C17, C20, C22
22	34.80	1.83 (1H, m), 1.62 (1H, m)	H23	C22	-
23	26.40	1.81 (2H, m)	H22/H24	C23	-
24	86.40	3.57 (1H, dd, 4.6, 9.4)	H23	C24	-
25	70.30	-	-	-	-
26	27.80	1.13 (3H, s)	-	C26	C24, C25
27	24.10	1.05 (3H, s)	-	C27	C24, C25
28	26.80	1.02 (3H, s)	-	C28	C3, C4, C5
29	21.00	0.97 (3H, s)	-	C29	C3, C4, C5
30	16.30	0.82 (3H, s)	-	C30	C8, C13, C14, C15

Cabraleone (2). Colorless needle crystal, m.p. 160–161 °C, IR ν_{max} (cm^{-1}): 3584, 2964, 1708, 1386, 1369, 1058; ^{1}H-NMR ($CDCl_3$, 500 MHz) and ^{13}C-NMR spectral data ($CDCl_3$, 125 MHz) are shown in Table 2. HR-TOFMS *m/z* found at 459.3838 $[M+H]^+$ (calculated for $C_{30}H_{51}O_3$, *m/z* = 459.3838).

Cabralealactone (3). Colorless crystal, m.p. 157–159 °C, IR ν_{max} (cm^{-1}): 2972, 1755, 1704, 1386, 1376, 1084. ^{1}H-NMR, δ_H (ppm): 1.78 (1H, dd, *J* = 7.8, 2.5 Hz, H-1a), 1.42 (1H, d, *J* = 7.8 Hz, H-1b), 2.57 (1H, dd, *J* = 8.5, 3.0 Hz, H-2a), 2.44 (1H, dd, *J* = 8.5, 4.2 Hz, H-2b), 1.32 (1H, t, *J* = 6.3 Hz, H-5), 1.57 (1H, ddd, *J* = 7.5, 6.3, 2.8 Hz, H-6a), 1.51 (1H, dd, *J* = 6.3, 2.8 Hz, H-6b), 1.52 (1H, dd, *J* = 9.0, 2.8 Hz, H-7a), 1.31 (1H, d, *J* = 9.0 Hz, H-7b), 1.46 (1H, d, *J* = 5.6 Hz, H-9), 1.42 (1H, dd, *J* = 8.5, 2.7 Hz, H-11a), 1.13 (1H, ddd, *J* = 8.5, 4.5, 2.7 Hz, H-11b), 1.96 (1H, dd, *J* = 4.5, 2.7 Hz, H-12a), 1.27 (1H, ddd, *J* = 7.8, 4.5, 2.7 Hz, H-12b), 1.57 (1H, dd, *J* = 4.5, 2.0 Hz, H-13), 1.51 (1H, ddd, *J* = 6.0, 4.5, 2.4 Hz, H-15a), 1.15 (1H, dd, *J* = 4.5, 2.4 Hz, H-15b), 1.86 (1H, dd, *J* = 7.0, 2.6 Hz, H-16a), 1.25 (1H, d, *J* = 7.0 Hz, H-16b), 1.17 (1H, dd, *J* = 5.6, 2.4 Hz, H-17), 0.94 (3H, s, Me-18), 1.00 (3H, s, Me-19), 1.37 (3H, s, Me-21), 2.14 (1H, m, H-22a), 1.90 (1H, m, H-22b), 2.65 (1H, m, H-23a), 2.51 (1H, m, H-23b), 1.08 (3H, s, Me-28), 1.04 (3H, s, Me-29), 0.90 (3H, s, Me-30); ^{13}C-NMR spectral data ($CDCl_3$, 125 MHz) are shown in Table 3. HR-TOFMS *m/z* found at 415.3229 $[M+H]^+$, (calculated for $C_{27}H_{43}O_3$, *m/z* = 415.3212).

Eichlerianic acid (4). White crystal, m.p. 165–167 °C, IR ν_{max} (cm^{-1}): 3421, 2968, 1704, 1376, 1260. ^{1}H-NMR: δ_H (ppm): 1.97 (1H, ddd, *J* = 8.5, 6.0, 3.5 Hz, H-1a), 1.53 (1H, dd, *J* = 6.0, 3.5 Hz, H-1b), 2.39 (1H, dd, *J* = 7.8, 3.5 Hz, H-2a), 2.18 (1H, ddd, *J* = 7.8, 6.2, 3.5 Hz, H-2b), 1.96 (1H, dd, *J* = 8.1, 5.6 Hz, H-5), 1.87 (2H, d, *J* = 5.6 Hz, H-6), 1.35 (2H, dd, *J* = 6.8, 5.6 Hz, H-7), 1.45 (1H, dd, *J* = 6.4, 3.2 Hz, H-9), 1.41 (2H, d, *J* = 6.4 Hz, H-11), 1.62 (1H, dd, *J* = 7.3, 4.0 Hz, H-13), 1.43 (2H, dd, *J* = 8.2, 3.5 Hz, H-15), 1.78 (2H, dd, *J* = 7.8, 3.5 Hz, H-16), 1.81 (1H, ddd, *J* = 7.8, 3.5, 2.1 Hz, H-17), 0.89 (3H, s, Me-18), 0.86 (3H, s, Me-19), 1.15 (3H, s, Me-21), 1.54 (2H, d, *J* = 6.4 Hz, H-22), 1.86 (2H, d, *J* = 6.4 Hz, H-23), 3.64 (1H, d, *J* = 5.5 Hz, H-24), 1.20 (3H, s, Me-26), 1.12 (3H, s, Me-27), 4.85 (1H, s, H-28a), 4.66 (1H, s, H-28b), 1.73 (3H, s, Me-29), 1.02 (3H, s, Me-30); ^{13}C-NMR spectral data are shown in Table 3. HR-TOFMS *m/z* found at 475.3793 $[M+H]^+$, (calculated for $C_{30}H_{50}O_4$, *m/z* = 475.3787).

Table 3. NMR data of compounds **3–5*** in $CDCl_3$ (δ in ppm, 125 MHz ^{13}C-NMR)

Position of Carbon	**3** δ_C	**4** δ_C	**5** δ_C
1	39.90	34.30	39.00
2	34.10	28.20	27.50
3	218.00	179.30	78.90
4	47.40	147.50	38.90
5	55.30	50.80	55.80
6	19.60	24.60	18.30
7	34.60	33.90	35.20
8	40.30	40.00	40.40
9	50.20	41.20	50.60
10	36.90	39.10	37.10
11	21.90	22.30	21.50
12	31.00	26.90	24.90
13	43.30	42.90	42.40
14	50.10	50.40	50.30
15	31.20	31.50	31.20
16	26.80	25.80	27.50
17	49.20	49.70	50.10
18	16.10	16.30	15.50
19	15.20	20.20	16.20
20	90.00	86.60	75.10
21	25.50	27.20	25.40
22	25.00	34.70	36.60
23	29.20	26.40	29.20
24	176.70	86.40	76.50
25	-	70.30	147.70
26	-	27.90	110.90
27	-	23.20	17.80
28	26.80	113.50	28.00
29	21.00	24.00	15.40
30	16.00	15.30	16.50

(+)-Fouquierol (5). White colorless crystals, m.p. 147–149 °C, IR ν_{max} (cm^{-1}): 3422, 2945, 1708, 1635, 1376, 1084. ^{1}H-NMR, δ_H (ppm): 1.68 (1H, ddd, *J* = 6.0, 4.5, 2.8 Hz, H-1a), 1.03 (1H, dd, *J* = 4.5, 2.8 Hz, H-1b), 1.65 (1H, ddd, *J* = 7.8, 4.5, 3.4 Hz, H-2a), 1.57 (1H, dd, *J* = 4.5, 3.4 Hz, H-2b), 3.20 (1H, dd, *J* = 6.4, 4.5 Hz, H-3), 0.74 (1H, ddd, *J* = 7.8, 6.4, 2.6 Hz, H-5), 1.54 (1H, ddd, *J* = 7.8, 5.8, 2.5 Hz, H-6a), 1.45 (1H, dd, *J* = 5.8, 2.5 Hz, H-6b), 1.52

(1H, dd, *J* = 6.8, 2.5 Hz, H-7a), 1.29 (1H, d, *J* = 6.8 Hz, H-7b), 1.33 (1H, dd, *J* = 8.5, 4.8 Hz, H-9), 1.49 (1H, ddd, *J* = 9.2, 4.8, 3.4 Hz, H-11a), 1.26 (1H, dd, *J* = 4.8, 3.4 Hz, H-11b), 1.68 (1H, ddd, *J* = 7.9, 4.8, 3.4 Hz, H-12a), 1.46 (1H, dd, *J* = 4.8, 3.4 Hz, H-12b), 1.68 (1H, dd, *J* = 4.8, 1.8 Hz, H-13), 1.46 (1H, ddd, *J* = 8.0, 5.6, 3.2 Hz, H-15a), 1.08 (1H, dd, *J* = 5.6, 3.2 Hz, H-15b), 1.65 (1H, dd, *J* = 6.7, 3.2 Hz, H-16a), 1.57 (1H, ddd, *J* = 7.8, 6.7, 3.2 Hz, H-16b), 1.66 (1H, dd, *J* = 6.7, 3.2 Hz, H-17), 0.96 (3H, s, Me-18), 0.84 (3H, s, Me-19), 1.15 (3H, s, Me-21), 1.47 (1H, d, *J* = 8.9 Hz, H-22a), 1.29 (1H, dd, *J* = 8.9, 4.1 Hz, H-22b), 1.29 (2H, d, *J* = 8.9 Hz, H-23), 4.04 (1H, t, *J* = 6.1 Hz, H-24), 4.96 (1H, s, H-26a), 4.84 (1H, s, H-26b), 1.74 (3H, s, Me-27), 0.97 (3H, s, Me-28), 0.77 (3H, s, Me-29), 0.88 (3H, s, Me-30); ^{13}C-NMR spectral data are shown in Table 3. HR-TOFMS *m/z* found at 483.3823 $[M+Na]^+$ (calculated for $C_{30}H_{52}O_3Na$, *m/z* = 483.3814).

Cytotoxic activity test by Presto Blue assay

Using the Presto Blue cell viability assay, the cytotoxic effect of compounds against A549 lung cancer cells was evaluated. This technique was formerly described by Hutagaol et al. [35]. Cells were cultivated in 96-well microliter plates at a density of 1.7×10^4 cells per well for 24 h in RPMI 1640 media supplemented with 10% (v/v) FBS and 1 L/mL antibiotics. The compounds were introduced to the wells after 24 h. Viability was determined after 96 h by observing the metabolic conversion reduction of resazurin substrate into the pink fluorescent resorufin product produced by viable cells. Using a multimode reader, the Presto Blue assay results were read at 570 nm and the reference at 600 nm. The following concentrations of each compound were tested in DMSO: 3.91, 7.81, 15.63, 31.25, 62.50, 125.00, 250.00, and 500.00 g/mL, with a final concentration of 2% in each well: 3.91, 7.81, 15.63, 31.25, 62.50, 125.00, 250.00, and 500.00 g/mL. Using the linear regression method in Microsoft Excel, IC_{50} values were calculated following two parallel experiments of each compound concentration. Doxorubicin served as the positive experimental control in this study.

■ RESULTS AND DISCUSSION

Five triterpenoid compounds (Fig. 1) were obtained by separating and purifying the *n*-hexane extract from the stem bark of *A. cucullata* using the column chromatography technique.

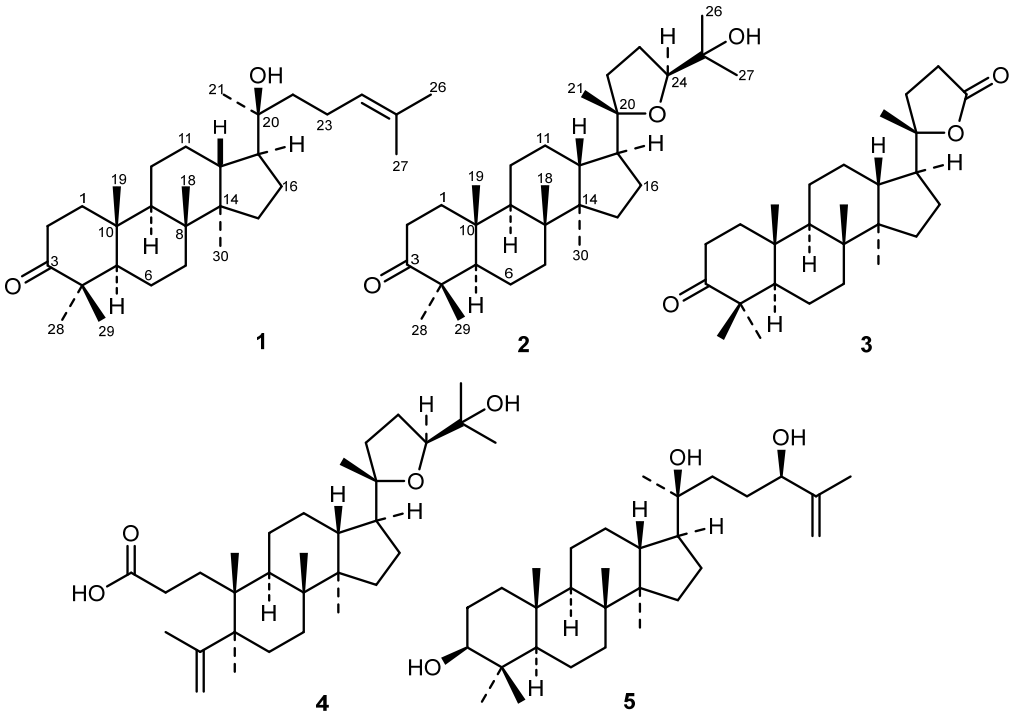

Fig 1. Structures of triterpenoids **1**–**5**

Compound **1** was isolated as a colorless white crystal. The molecular formula of **1** was determined on HR-TOF-ESI-MS, giving a molecular formula of $C_{30}H_{50}O_2$ (Fig. S1) with *m/z* = 443.3817 as $[M+H]^+$ (calculated *m/z* for $C_{30}H_{51}O_2$ 443.3811), corresponding to six degrees of unsaturation. The IR spectrum (Fig. S2) displayed the existence of hydroxyl (3448 cm^{-1}), aliphatic C–H sp^3 (2955 cm^{-1}), carbonyl (1704 cm^{-1}), ether (1018 cm^{-1}), and *gem*-dimethyl (1378 cm^{-1}) functionalities. The ^{1}H-NMR spectrum (Fig. S3) showed the presence of eight methyls singlet at δ_H/ppm 0.82 (CH_3-30), 0.87 (CH_3-19), 0.93 (CH_3-18), 0.97 (CH_3-29), 1.01 (CH_3-28), 1.08 (CH_3-21), 1.56 (CH_3-27), and 1.62 (CH_3-26), and an olefinic methine at δ_H/ppm 5.05 (1H, t, *J* = 5.0 Hz, H-24). Thirty carbons were revealed through ^{13}C-NMR (Fig. S4) and DEPT (Fig. S5) experiments, which were classified as eight methyls at δ_C/ppm 15.2 (C-18), 16.0 (C-19), 16.4 (C-30), 17.7 (C-27), 21.0 (C-29), 25.5 (C-21), 25.7 (C-26), and 26.7 (C-28), ten methylenes at δ_C/ppm 19.7 (C-6), 22.0 (C-11), 22.6 (C-23), 24.8 (C-16), 27.5 (C-12), 31.2 (C-15), 34.1 (C-2), 34.6 (C-7), 39.9 (C-1), and 40.5 (C-22), four methines (including one sp^2) at δ_C/ppm 124.7 (C-24), 42.4 (C-13), 49.8 (C-17), 50.0 (C-9), and 55.4 (C-5), six quaternary carbons (with two of them are one sp^2 and one oxygenated sp^3 carbons) at δ_C/ppm 131.6 (C-25), 75.4 (C-20), 36.8 (C-10), 40.3 (C-8), 47.4 (C-4), and 50.3 (C-14), and one carbonyl carbon at δ_C/ppm 218.0 (C-3). In the HSQC spectrum data (Fig. S6) presented in Table 1, the proton signals were connected directly to their carbon atoms. The existence of two unsaturated degrees in the primary data indicated that compound **1** was a triterpenoid with a tetracyclic structure. This hypothesis was strengthened by the presence of four aliphatic quaternary carbons devoid of oxygen. The planar structure of **1** was analyzed through the 2D NMR spectra. The ^{1}H-^{1}H COSY spectrum of **1** (Fig. S7) revealed key coupling relationships of H_1/H_2, $H_5/H_6/H_7$, $H_9/H_{11}/H_{12}/H_{13}/H_{17}$, $H_{15}/H_{16}/H_{17}$, $H_{22}/H_{23}/H_{24}$, together with the HMBC correlations (Fig. S8a and S8b) from CH_3-18 to C-7, C-8, C-9; CH_3-19 to C-1, C-5, C-9, C-10; CH_3-30 to C-8, C-13, C-14, C-15; CH_3-28/CH_3-29 to C-3, C-4, C-5, showing that **1** possessed a tetracyclic of the dammarane-type skeleton with the presence of carbonyl at C-3. Furthermore, the hydroxyl attachment at C-20 and olefinic group at C-24/25 in the side chain of **1** was deduced by correlations of CH_3-21 to C-17, C-20, H-22 to C-20, CH_3-26/CH_3-27 to C-24, C-25, and H-22 to C-24. Compound **1** showed δ_C/ppm 75.4 (C-20), 25.5 (C-21), and 40.5 (C-22), which is identical to the 20*S* [43]. Additional analysis and a review of the literature confirmed that compound **1** was (20*S*)-20-hydroxydammar-24-en-3-one compared to those previously reported [44], which was at first isolated from the genus of *Aglaia*.

Compound **2** was acquired as a colorless needle crystal. The molecular formula of **2** was determined as $C_{30}H_{50}O_3$ with six degrees of unsaturation by the analysis of its positive HR-TOF-ESI-MS (Fig. S9) *m/z* = 459.3838 as $[M+H]^+$, calculated for $C_{30}H_{51}O_3$ *m/z* = 459.3838. The IR spectrum (Fig. S10) presented the existence of hydroxyl (3584 cm^{-1}), aliphatic C-H sp^3 (2964 cm^{-1}), carbonyl (1708 cm^{-1}), ether (1058 cm^{-1}), and *gem*-dimethyl (1386 and 1369 cm^{-1}) groups. The ^{1}H-NMR spectrum (Fig. S11) showed the existence of eight methyls singlet at δ_H/ppm 0.82 (CH_3-30), 0.88 (CH_3-19), 0.94 (CH_3-18), 1.01 (CH_3-28), 1.05 (CH_3-27), 1.08 (CH_3-21), and 1.12 (CH_3-26), and one oxygenated methine at δH/ppm 3.57 (1H, dd, *J* = 5.0, 10.0 Hz, H-24). The ^{13}C-NMR (Fig. S12) and DEPT 135° (Fig. S13) spectra of **2** exhibited 30 carbon resonances, including eight methyls at δ_C/ppm 15.2 (C-18), 16.1 (C-19), 16.3 (C-20), 21.0 (C-29), 24.1 (C-27), 26.8 (C-28), 27.1 (C-21), and 27.8 (C-26), ten methylenes at δ_C/ppm 19.7 (C-6), 22.3 (C-11), 25.8 (C-16), 26.4 (C-23), 27.0 (C-12), 31.4 (C-15), 34.1 (C-2), 34.6 (C-7), 34.8 (C-22), and 39.9 (C-1), five methines sp^3 (involving one oxygenated) at δ_C/ppm 86.4 (C-24), 43.0 (C-13), 49.8 (C-17), 50.2 (C-9), and 55.3 (C-5), six quaternary carbons sp^3 (with two of them are oxygenated carbons) at δ_C/ppm 70.3 (C-25), 86.5 (C-20), 36.9 (C-10), 40.3 (C-8), 47.4 (C-4), and one carbonyl carbon at δ_C/ppm 218.0 (C-3). The above data possessed two degrees of unsaturation (one ketone carbonyl and one cyclic by a tetrahydrofuran moiety [45]), indicating four tetracyclic of a triterpenoid framework. The ^{1}H-^{1}H COSY (Fig. S15) correlations of H_1/H_2, $H_5/H_6/H_7$, $H_9/H_{11}/H_{12}/H_{13}/H_{17}$, $H_{15}/H_{16}/H_{17}$ allowed the structural skeleton that is dammarane typed. The HMBC spectrum

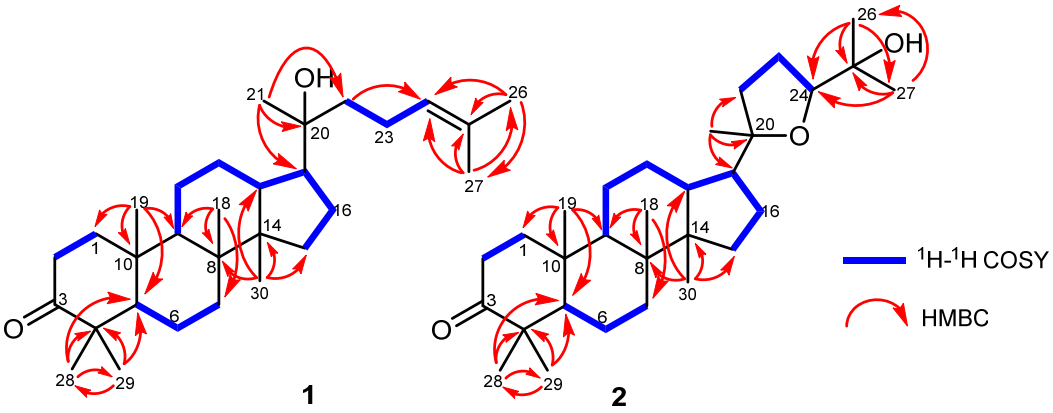

Fig 2. Selected HMBC and ^{1}H-^{1}H COSY correlations of compounds **1** and **2**

(Fig. S16), shows strong correlations (Fig. 2) from CH_3-18 to C-7, C-8, C-9; CH_3-19 to C-1, C-5, C-9, C-10; CH_3-30 to C-8, C-13, C-14, C-15; and CH_3-28/ CH_3-29 to C-3, C-4, C-5 proved the presence of a tetracyclic dammarane-type, as well as the ketonic group positioned at C-3 in **2**. Furthermore, the tetrahydrofuran form in the side chain of **2** was determined through the correlations of CH_3-21 to C-17, C-20, C-22, and CH_3-26/CH_3-27 to C-24, C-25, together with ^{1}H-^{1}H COSY correlations of H_{22}/H_{23}/H_{24} as demonstrated in Fig. 2. Compound **2** provided the chemical shifts of [δ_C/ppm 86.4 (C-24), δ_H/ppm 3.57 (1H, dd, *J* = 5.0, 10.0, H-24)] and [δ_C/ppm 86.5 (C-20)], referencing to the 20*S* and 24*S* orientations [45-46]. The NMR data comparison of compound **2** with the literature [47] revealed that **2** was cabraleone or 20*S*,24*S*-epoxy-25-hydroxydammar-3-one, which was isolated from *A. cucullata* for the first time.

Compound **3** was obtained as a colorless crystal. The molecular formula of **3** was verified as $C_{27}H_{42}O_3$ based on HR-TOF-ESI-MS (Fig. S17) *m/z* = 415.3229 as $[M+H]^+$, calculated for $C_{27}H_{43}O_3$ *m/z* = 415.3212, which described seven degrees of unsaturation. The IR spectrum (Fig. S18) displayed the existence of aliphatic C-H sp^3 (2972 cm^{-1}), carbonyl ester (1755 cm^{-1}), carbonyl ketone (1704 cm^{-1}), *gem*-dimethyl (1386 and 1376 cm^{-1}), and ether group (1084 cm^{-1}). The ^{1}H-NMR spectrum (Fig. S19) showed the presence of six methyls singlet at δH/ppm 0.90 (CH_3-30), 0.94 (CH_3-18), 1.00 (CH_3-19), 1.04 (CH_3-29), 1.08 (CH_3-28), and 1.37 (CH_3-21). These data implied that the oxidative degradation of two side chain methyl groups led to the γ-lactone moiety, resulting in the formation of tris *nor*-triterpenoid compound [48]. The ^{13}C-NMR (Fig. S20) and DEPT 135° (Fig. S21) of **3** exhibited of 27 carbons, assignable to six methyls at δ_C/ppm 15.2 (C-19), 16.0 (C-30), 16.2 (C-18), 21.0 (C-29), 25.5 (C-21), and 26.7 (C-28), 10 methylenes at δ_C/ppm 19.6 (C-6), 21.9 (C-11), 25.0 (C-22), 26.8 (C-16), 29.2 (C-23), 31.0 (C-12), 31.2 (C-15), 34.1 (C-2), 34.5 (C-7), and 39.9 (C-1), four methines sp^3 at δ_C/ppm 43.3 (C-13), 49.3 (C-17), 49.9 (C-9), and 55.3 (C-5), five quaternary carbons sp^3 (including one oxygenated carbon) at δ_C/ppm 90.1 (C-20), 36.8 (C-10), 40.3 (C-8), 47.4 (C-12), and 50.1 (C-14), one carbonyl ester carbon at δ_C/ppm 176.8 (C-24), and one carbonyl ketone carbon at δ_C/ppm 218.0 (C-3). Based on the ^{1}H-NMR, ^{13}C-NMR, DEPT 135° spectra, corresponding to the literature [49], compound **3** was established as the known compound cabralealactone, which was isolated for the first time in the *A. cucullata*.

Compound **4** was isolated as a white crystal. The molecular formula of **4** was determined on HR-TOF-ESI-MS, giving a molecular formula of $C_{30}H_{50}O_4$ (Fig. S22) with *m/z* 475.3793 $[M+H]^+$ (calculated *m/z* of $C_{30}H_{51}O_4$ = 475.3787), which revealed six degrees of unsaturation. The IR spectrum (Fig. S23) displayed the existence of hydroxyl (3421 cm^{-1}), aliphatic C-H sp^3 (2968 cm^{-1}), carbonyl ketone (1704 cm^{-1}), *gem*-dimethyl (1376 cm^{-1}), and ether group (1260 cm^{-1}). The ^{1}H-NMR spectrum (Fig. S24) showed the presence of seven methyls singlet at δ_H/ppm 0.86 (CH_3-19), 0.89 (CH_3-18), 1.02 (CH_3-30), 1.12 (CH_3-27), 1.15 (CH_3-21), 1.20 (CH_3-

26), and 1.73 (CH_3-19). The presence of one oxygenated methine in the tetrahydrofuran ring at δ_H/ppm 3.64 (1H, dd, J = 5.5, 9.5 Hz, H-24), and one methylene sp^2 at [δ_H/ppm 4.85 (1H, s, H-28a), 4.66 (1H, s, H-28b)], which are characteristic for a *seco*-dammarane triterpenoid [50]. Compound **4** possessed 30 carbons (Fig. S25 and S26), corresponding to seven methyls at δ_C/ppm 15.3 (C-30), 16.3 (C-18), 20.2 (C-19), 23.2 (C-27), 24.0 (C-29), 27.2 (C-21), and 27.9 (C-26), 11 methylenes (including one sp^2) at δ_C/ppm 113.5 (C-28), 22.3 (C-11), 24.6 (C-6), 25.8 (C-16), 26.4 (C-23), 26.9 (C-12), 28.2 (C-2), 31.5 (C-15), 33.9 (C-7), 34.3 (C-1), and 34.7 (C-22), five methines sp^3 (involving one oxygenated) at δ_C/ppm 86.4 (C-24), 41.2 (C-9), 42.9 (C-13), 49.7 (C-17), and 50.8 (C-5), six quaternary carbons (including one olefinic and two oxygenated) at δ_C/ppm 147.5 (C-4), 70.3 (C-25), 86.6 (C-20), 39.1 (C-10), 40.0 (C-8), and 50.4 (C-14), and one carbonyl of carboxylic acid at δ_C/ppm 179.8 (C-3). Based on the ^{1}H-NMR, ^{13}C-NMR, DEPT 135° spectra, which well-matched with the literature [50], compound **4** was confirmed as the known compound eichlerianic acid, which was isolated for the first time in the *A. cucullata*.

Compound **5** was isolated as a colorless white crystal. Its molecular formula was determined as $C_{30}H_{52}O_3$ with six degrees of unsaturation by the analysis of its positive HR-TOF-ESI-MS (Fig. S27) m/z = 483.3823 as $[M+Na]^+$, calculated for $C_{30}H_{52}O_3Na$ m/z = 483.3814. The IR spectrum (Fig. S28) displayed the existence of hydroxyl (3422 cm^{-1}), aliphatic C-H sp^3 (2945 cm^{-1}), carbonyl ketone (1708 cm^{-1}), olefinic (1635 cm^{-1}), *gem*-dimethyl (1376 cm^{-1}), and ether group (1084 cm^{-1}). The ^{1}H-NMR spectrum (Fig. S29) showed the presence of seven methyls singlet at δ_H/ppm 0.77 (CH_3-29), 0.84 (CH_3-19), 0.88 (CH_3-30), 0.96 (CH_3-18), 0.97 (CH_3-28), 1.15 (CH_3-21), and 1.73 (CH_3-27), two oxygenated methines at δ_H/ppm 3.20 (1H, m, H-3), and 4.04 (1H, t, J = 6.1 Hz, H-24), and one methylene sp^2 at [δ_H/ppm 4.96 (1H, s, H-27a), 4.84 (1H, s, H-27b)]. The ^{13}C-NMR (Fig. S30) and DEPT 135° (Fig. S31) spectra of **5** revealed 30 carbon resonances, including seven methyls at δ_C/ppm 15.4 (C-29), 15.5 (C-18), 16.2 (C-19), 16.5 (C-30), 17.8 (C-27), 25.4 (C-21), and 28.0 (C-28), 11 methylenes (involving one olefinic sp^2) at δ_C/ppm 110.9 (C-26), 18.3 (C-6), 21.5 (C-11), 24.9 (C-12), 27.4 (C-2), 27.5 (C-16), 29.2 (C-23), 31.2 (C-15), 35.2 (C-7), 36.6 (C-22), and 39.0 (C-1), six methines sp^3 (including two oxygenated) at δ_C/ppm 76.5 (C-24), 78.9 (C-3), 42.4 (C-13), 50.1 (C-17), 50.6 (C-9), and 55.8 (C-5), six quaternary carbons (including one olefinic sp^2 and one oxygenated sp^3) at δ_C/ppm 147.7 (C-25), 75.1 (C-20), 37.1 (C-10), 38.9 (C-4), 40.4 (C-8), and 50.3 (C-14). Based on the ^{1}H-NMR, ^{13}C-NMR, and DEPT 135° spectra of compound **5** revealed a good fit to the literature [51], compound **5** was confirmed as the known compound (+)-fouquierol, which was isolated for the first time in the Meliaceae family and *Aglaia* genus.

All isolated compounds **1**–**5** were classified as dammarane-type triterpenoids. In *Aglaia* genus, dammarane-type triterpenoids were commonly found. The modification of dammarane-type triterpenoids, including the A ring opening (such as in compound **4**) and formation of epoxide ring at C-20/C-24 (such as in compounds **2** and **4**), also followed by degradation of three carbon atoms in the side chain to give lactone ring (such as in compound **3**), usually can be found in other species of Aglaia genus [45,48]. The cytotoxic activity of the triterpenoids **1**–**5** was assayed against the A549 lung cancer cell (Table 4) using a method previously reported [52-53]. Doxorubicin (1.08 µg/mL) was used as the positive experimental control in this study. Among all triterpenoid compounds, eichlerianic acid (**4**) had the highest cytotoxic activity, whereas (+)-fouquierol (**5**) showed the lowest cytotoxic activity. Compounds **1** (IC_{50} 142.30 µM) and **4** (IC_{50} 32.17 µM) displayed moderate cytotoxic activity, compounds **2** (IC_{50} 316.40 µM) and **3** (IC_{50} 415.43 µM) showed weak cytotoxic activity, and compound **5** (IC_{50} 1747.63 µM) showed no cytotoxic activity [54]. The IC_{50} value implicated that the existence

Table 4. Cytotoxic activity of compounds **1**–**5**

Compounds	IC_{50} (µM)
(20*S*)-20-hydroxydammar-24-en-3-one (**1**)	142.30
Cabraleone (**2**)	316.40
Cabralealactone (**3**)	415.43
Eichlerianic acid (**4**)	32.17
(+)-fouquierol (**5**)	1747.63
Doxorubicin (+)	1.08

of a *seco* ring in compound **4** greatly enhanced its cytotoxic activity compared to compound **2**. Furthermore, compound **1** had stronger cytotoxic activity than compound **5**, demonstrating that the presence of an olefinic terminal with hydroxyl at C-24 in compound **5** reduced its cytotoxic activity. These findings suggest that the *seco* moiety in the A ring and *gem*-dimethyl attached to quaternary carbon sp^2 at the aliphatic side chain structure play several critical structural features in the cytotoxic activity of dammarane-type triterpenoids.

CONCLUSION

The *n*-hexane preparation of *A. cucullata* stems bark produced five dammarane-type triterpenoids, which were identified as (20*S*)-20-hydroxydammar-24-en-3-one (**1**), cabraleone (**2**), cabralealactone (**3**), eichlerianic acid (**4**), and (+)-fouquierol (**5**). Both compounds **1** and **5** were isolated for the first time from the Meliaceae family and the *Aglaia* genus, respectively. Compound **1** was the first compound to be isolated from the *Aglaia* genus. The cytotoxic potential of substances **1** through **5** was investigated using the A549 lung cancer cell type as a test subject. Among the triterpenoids of the dammarane class, Compound **4** exhibited the highest level of activity, whereas Compound **5** exhibited the lowest level. Increased cytotoxicity in the triterpenoid dammarane type can be attributed to the presence of a *seco* component in the A ring as well as *gem*-dimethyl connected to quaternary carbon sp^2 in the aliphatic side chain. Because of this, the identification of these compounds lays the groundwork for the use of triterpenoid dammarane-type compounds as a therapeutic possibility for the treatment of lung cancer. These compounds have the potential to be developed into lead compounds for the treatment of lung cancer.

ACKNOWLEDGMENTS

This study was financially supported by the Ministry of Education and Culture, Innovative and Research Council, Indonesia, Master Thesis Research (PTM) Grant (No. 1318/UN6.3.1/PT.00/2022) and RKDU 2019 by Desi Harneti.

REFERENCES

[1] Shang, Y., and Huang, S., 2019, Multi-omics data-driven investigations of metabolic diversity of plant triterpenoids, *Plant J.*, 97 (1), 101–111.

[2] Chen, Y., Zhou, B., Li, J., Tang, H., Tang, J., and Yang, Z., 2018, Formation and change of chloroplast-located plant metabolites in response to light conditions, *Int. J. Mol. Sci.*, 19 (3), 654.

[3] Zheng, X., Luo, X., Ye, G., Chen, Y., Ji, X., Wen, L., Xu, Y., Xu, H., Zhan, R., and Chen, W., 2015, Characterisation of two oxidosqualene cyclases responsible for triterpenoid biosynthesis in *Ilex asprella*, *Int. J. Mol. Sci.*, 16 (2), 3564–3578.

[4] Ren, Y., and Kinghorn, A.D., 2019, Natural product triterpenoids and their semi-synthetic derivatives with potential anticancer activity, *Planta Med.*, 85 (11/12), 802–814.

[5] Lim, H.J., Bak, S.G., Lim, H.J., Lee, S.W., Lee, S., Ku, S.K., Park, S.I., Lee, S.J., and Rho, M.C., 2020, Acyclic triterpenoid isolated from *Alpinia katsumadai* alleviates formalin-induced chronic mouse paw inflammation by inhibiting the phosphorylation of ERK and NF-κB, *Molecules*, 25 (15), 3345.

[6] Li, J., Ni, G., Li, L., Liu, Y., Mai, Z., Wang, R., and Yu, D., 2019, New iridal-type triterpenoid derivatives with cytotoxic activities from *Belamcanda chinensis*, *Bioorg. Chem.*, 83, 20–28.

[7] An, X., Wang, J., Yu, X., Wu, H., and Liu, W., 2022, Two new polypodane-type bicyclic triterpenoids from mastic, *Open Chem.*, 20 (1), 267–271.

[8] Stonik, V.A., and Kolesnikova, S.A., 2021, Malabaricane and isomalabaricane triterpenoids, including their glycoconjugated forms, *Mar. Drugs*, 19 (6), 327.

[9] Song, M., Chan, G., Lin, L.G., Li, D., Zhang, K., Zhang, X.Q., Ye, W.C., Li, N., and Zhang, Q.W., 2022, Triterpenoids from the fruits of *Melia azedarach* L. and their cytotoxic activities, *Phytochemistry*, 201, 113280.

[10] Saptanti, K., Heliawati, L., Hermawati, E., and Syah, Y.M., 2022, Pentacyclic triterpenes from the leaves

extract of *Sandoricum koetjape*, *J. Nat. Med.*, 76 (4), 842–848.

[11] Wang, Y.R., Yu, Y., Li, S.M., Liu, W., Li, W., Morris-Natschke, S.L., Goto, M., Lee, K.H., and Huang, X.F., 2018, Salvisertin A, a new hexacyclic triterpenoid, and other bioactive terpenes from *Salvia deserta* root, *Chem. Biodiversity*, 15 (4), e1800019.

[12] Ouyang, X.L., Qin, F., Huang, R.Z., Liang, D., Wang, C.G., Wang, H.S., and Liao, Z.X., 2019, NF-κB inhibitory and cytotoxic activities of hexacyclic triterpene acid constituents from *Glechoma longituba*, *Phytomedicine*, 63, 153037.

[13] Teixeira, F.S., Vidigal, S.S.M.P., Pimentel, L.L., Costa, P.T., Tavares-Valente, D., Azevedo-Silva, J., Pintado, M.E., Fernandes, J.C., and Rodríguez-Alcalá, L.M., 2021, Phytosterols and novel triterpenes recovered from industrial fermentation coproducts exert *in vitro* anti-inflammatory activity in macrophages, *Pharmaceuticals*, 14 (6), 583.

[14] Zhang, J., Zhang, Q., Xu, Y., Li, H., Wang, C., Liu, Z., Liu, P., Liu, Y., Meng, Q., Zhao, F., and Zhao, F., 2019, Synthesis and *in vitro* anti-inflammatory activity of C20 epimeric ocotillol-type triterpenes and protopanaxadiol, *Planta Med.*, 85 (4), 292–301.

[15] Muhammad, D., Hubert, J., Lalun, N., Renault, J.H., Bobichon, H., Nour, M., and Voutquenne-Nazabadioko, L., 2015, Isolation of flavonoids and triterpenoids from the fruits of *Alphitonia neocaledonica* and evaluation of their anti-oxidant, antityrosinase and cytotoxic activities, *Phytochem. Anal.*, 26 (2), 137–144.

[16] Oprean, C., Zambori, C., Borcan, F., Soica, C., Zupko, I., Minorics, R., Bojin, F., Ambrus, R., Muntean, D., Danciu, C., Pinzaru, I.A., Dehelean, C., Paunescu, V., and Tanasie, G., 2016, Anti-proliferative and antibacterial *in vitro* evaluation of the polyurethane nanostructures incorporating pentacyclic triterpenes, *Pharm. Biol.*, 54 (11), 2714–2722.

[17] Hisham Shady, N., Youssif, K.A., Sayed, A.M., Belbahri, L., Oszako, T., Hassan, H.M., and Abdelmohsen, U.R., 2021, Sterols and triterpenes: Antiviral potential supported by *in-silico* analysis, *Plants*, 10 (1), 41.

[18] Innocente, A., Casanova, B.B., Klein, F., Lana, A.D., Pereira, D., Muniz, M.N., Sonnet, P., Gosmann, G., Fuentefria, A.M., and Gnoatto, S.C.B., 2014, Synthesis of isosteric triterpenoid derivatives and antifungal activity, *Chem. Biol. Drug Des.*, 83 (3), 344–349.

[19] Nazaruk, J., and Borzym-Kluczyk, M., 2015, The role of triterpenes in the management of diabetes mellitus and its complications, *Phytochem. Rev.*, 14 (4), 675–690.

[20] Xu, G.B., Xiao, Y.H., Zhang, Q.Y., Zhou, M., and Liao, S.G., 2018, Hepatoprotective natural triterpenoids, *Eur. J. Med. Chem.*, 145, 691–716.

[21] Yu, C.X., Wang, R.Y., Qi, F.M., Su, P.J., Yu, Y.F., Li, B., Zhao, Y., Zhi, D.J., Zhang, Z.X., and Fei, D.Q., 2019, Eupulcherol A, a triterpenoid with a new carbon skeleton from: *Euphorbia pulcherrima*, and its anti-Alzheimer's disease bioactivity, *Org. Biomol. Chem.*, 18 (1), 76–80.

[22] Renda, G., Gökkaya, İ., and Şöhretoğlu, D., 2022, Immunomodulatory properties of triterpenes, *Phytochem. Rev.*, 21 (2), 537–563.

[23] Lehbili, M., Alabdul Magid, A., Kabouche, A., Voutquenne-Nazabadioko, L., Abedini, A., Morjani, H., Gangloff, S.C., and Kabouche, Z., 2018, Antibacterial, antioxidant and cytotoxic activities of triterpenes and flavonoids from the aerial parts of *Salvia barrelieri* Etl, *Nat. Prod. Res.*, 32 (22), 2683–2691.

[24] Jang, E., and Lee, J.H., 2021, Promising anticancer activities of alismatis rhizome and its triterpenes via p38 and PI3k/Akt/mTOR signaling pathways, *Nutrients*, 13 (7), 2455.

[25] Nogueira, T.S.R., Passos, M.S., Nascimento, L.P.S., Arantes, M.B.S., Monteiro, N.O., Boeno, S.I.S., de Carvalho Junior, A., Azevedo, O.A., Terra, W.S., Vieira, M.G.C., Braz-Filho, R., and Curcino Vieira, I.J.C., 2020, Chemical compounds and biologic activities: A review of *Cedrela* genus, *Molecules*, 25 (22), 5401.

[26] Hamid, A.A., Aiyelaagbe, O.O., Negi, A.S., Kaneez, F., Luqman, S., Oguntoye, S.O., Kumar, S.B., and Zubair, M., 2018, Isolation and antiproliferative

activity of triterpenoids and fatty acids from the leaves and stem of *Turraea vogelii* Hook. f. ex benth, *Nat. Prod. Res*., 33 (2), 296–301.

[27] Happi, G.M., Kouam, S.F., Talontsi, F.M., Zühlke, S., Lamshöft, M., and Spiteller, M., 2015, Minor secondary metabolites from the bark of *Entandrophragma congoënse* (Meliaceae), *Fitoterapia*, 102, 35–40.

[28] Saleem, S., Muhammad, G., Hussain, M.A., and Bukhari, S.N.A., 2018, A comprehensive review of phytochemical profile, bioactives for pharmaceuticals, and pharmacological attributes of *Azadirachta indica*, *Phytother. Res*., 32 (7), 1241–1272.

[29] Hernandez, V., De Leo, M., Cotugno, R., Braca, A., De Tommasi, N., and Severino, L., 2018, New tirucallane-type triterpenoids from *Guarea guidonia*, *Planta Med.*, 84 (9/10), 716–720.

[30] Matsumoto, T., Kitagawa, T., Ohta, T., Yoshida, T., Imahori, D., Teo, S., bin Ahmad, H.S., and Watanabe, T., 2019, Structures of triterpenoids from the leaves of *Lansium domesticum*, *J. Nat. Med*., 73 (4), 727–734.

[31] Salam, S., Harneti, D., Maharani, R., Nurlelasari, N., Safari, A., Hidayat, A.T., Lesmana, R., Nafiah, M.A., Supratman, U., Kyle Prescott, T.A., and Shiono, Y., 2021, Cytotoxic triterpenoids from *Chisocheton pentandrus*, *Phytochemistry*, 187, 112759.

[32] Wang, W., Xia, Z., Tian, Z., Jiang, H., Zhan, Y., Liu, C., Li, C., and Zhou, H., 2020, Chemical constituents from the fruits of *Melia azedarach* (Meliaceae), *Biochem. Syst. Ecol.*, 92, 104094.

[33] Naini, A.A., Mayanti, T., and Supratman, U., 2022, Triterpenoids from *Dysoxylum* genus and their biological activities, *Arch. Pharmacal Res.*, 45 (2), 63–82.

[34] Zhang, L., Xia, J., Duan, Y., Wei, K., Gao, R., Li, D., Liu, X., Zhang, T., and Qiu, M., 2021, Toonamicrocarpavarin, a new tirucallane-type triterpenoid from *Toona ciliata*, *Nat. Prod. Res*., 35 (2), 266–271.

[35] Hutagaol, R.P., Harneti, D., Safari, A., Hidayat, A.T., Supratman, U., Awang, K., and Shiono, Y., 2021, Cytotoxic triterpenoids from the stem bark of *Aglaia angustifolia*, *J. Asian Nat. Prod. Res*., 23 (8), 781–788.

[36] Meepol, W., Maxwell, G.S., and Havanond, S., 2020, *Aglaia cucullata*: A little-known mangrove with big potential for research, *ISME/GLOMIS Electron. J*., 18 (1), 4–9.

[37] Duke, N., Sukardjo, S., and Kathiresan, K., 2010, *Aglaia cucullate*, *The IUCN Red List of Threatened Species*, https://www.iucnredlist.org/species/34364/9856175, Accessed on September 30th, 2022.

[38] Ahmed, F., Toume, K., Sadhu, S.K., Ohtsuki, T., Arai, M.A., and Ishibashi, M., 2010, Constituents of *Amoora cucullata* with TRAIL resistance-overcoming activity, *Org. Biomol. Chem*., 8 (16), 3696–3703.

[39] Pancharoen, R., Sommeechai, M., Maelim, S., Suanpaga, W., Srichaichana, J., Barber, P., and Dell, B., 2021, Phenology of urban trees in a tropical urban forest in Thailand, *Songklanakarin J. Sci. Technol.*, 43 (1), 87–95.

[40] Chumkaew, P., Kato, S., and Chantrapromma, K., 2006, Potent cytotoxic rocaglamide derivatives from the fruits of *Amoora cucullata*, *Chem. Pharm. Bull*., 54 (9), 1344–1346.

[41] DeFilipps, R.A., and Krupnick, G.A., 2018, The medicinal plants of Myanmar, *PhytoKeys*, 102, 1–341.

[42] Abdelfattah, M.S., Toume, K., Ahmed, F., Sadhu, S.K., and Ishibashi, M., 2010, Cucullamide, a new putrescine bisamide from *Amoora cucullata*, *Chem. Pharm. Bull.*, 58 (8), 1116–1118.

[43] Wang, K.C., Wang, P.H., and Lee, S.S., 1997, Microbial transformation of protopanaxadiol and protopanaxatriol derivatives with *Mycobacterium* sp. (NRRL B-3805), *J. Nat. Prod*., 60 (12), 1236–1241.

[44] Asai, T., and Fujimoto, Y., 2011, 2-Acety-1-(3-glycosyloxyoctadecanoyl)glycerol and dammarane triterpenes in the exudates from glandular trichome-like secretory organs on the stipules and leaves of *Cerasus yedoensis*, *Phytochem. Lett*., 4 (1), 38–42.

[45] Roux, D., Martin, M.T., Adeline, M.T., Sevenet, T., Hadi, A.H.A., and Païs, M., 1998, Foveolins A and

B, dammarane triterpenes from *Aglaia foveolata*, *Phytochemistry*, 49 (6), 1745–1748.

[46] Aalbersberg, W., and Singh, Y., 1991, Dammarane triterpenoids from *Dysoxylum richii*, *Phytochemistry*, 30 (3), 921–926.

[47] Hisham, A., Ajitha Bai, M.D., Fujimoto, Y., Hara, N., and Shimada, H., 1996, Complete ^{1}H and ^{13}C NMR spectral assignment of cabraleadiol, a dammarane triterpene from *Dysoxylum malabaricum* Bedd, *Magn. Reson. Chem.*, 34 (2), 146–150.

[48] Oktaviani, D., Sukmawati, W., Farabi, K., Harneti, D., Nurlelasari, N., Darwati, D., Mahari, R., Mayanti, T., Safari, A., and Supratman, U., 2022, Terpenoids from the stem bark of *Aglaia elaeagnoidea* and their cytotoxic activity against HeLa and DU145 cancer cell lines, *Molekul*, 17 (1), 76–84.

[49] Phongmaykin, J., Kumamoto, T., Ishikawa, T., Suttisri, R., and Saifah, E., 2008, A new sesquiterpene and other terpenoid constituents of *Chisocheton penduliflorus*, *Arch. Pharmacal Res.*, 31 (1), 21–27.

[50] Kamarulzaman, F.A., Mohamad, K., Awang, K., and Lee, H.B., 2014, Chemical constituents of *Aglaia lanuginose*, *Pertanika J. Sci. Technol.*, 22 (1), 163–174.

[51] Ren, Y., Anaya-Eugenio, G.D., Czarnecki, A.A., Ninh, T.N., Yuan, C., Chai, H.B., Soejarto, D.D., Burdette, J.E., de Blanco, E.J.C., and Kinghorn, A.D., 2018, Cytotoxic and NF-κB and mitochondrial transmembrane potential inhibitory pentacyclic triterpenoids from *Syzygium corticosum* and their semi-synthetic derivatives, *Bioorg. Med. Chem.*, 26 (15), 4452–4460.

[52] Boncler, M., Rózalski, M., Krajewska, U., Podsędek, A., and Watala, C., 2014, Comparison of PrestoBlue and MTT assays of cellular viability in the assessment of anti-proliferative effects of plant extracts on human endothelial cells, *J. Pharmacol. Toxicol. Methods*, 69 (1), 9–16.

[53] Xu, M., Mccanna, D.J., and Sivak, J.G., 2015, Use of the viability reagent PrestoBlue in comparison with alamarBlue and MTT to assess the viability of human corneal epithelial cells, *J. Pharmacol. Toxicol. Methods*, 71, 1–7.

[54] Sajjadi, S.E., Ghanadian, M., Haghighi, M., and Mouhebat, L., 2015, Cytotoxic effect of *Cousinia verbascifolia* Bunge against OVCAR-3 and HT-29 cancer cells, *J. HerbMed Pharmacol.*, 4 (1), 15–19.

Supplementary Data

This supplementary data is a part of a paper entitled "Triterpenoids from the Stem Bark of *Aglaia cucullata* (Meliaceae) and Their Cytotoxic Activity against A549 Lung Cancer Cell Line".

Table of Contents

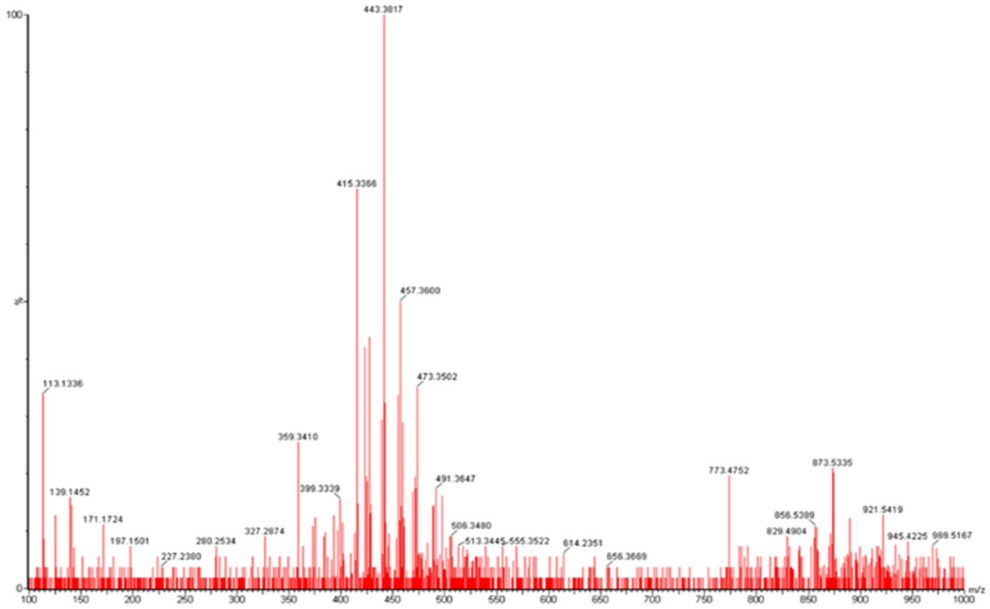

Fig S1. HR-TOFMS spectrum of (**1**)

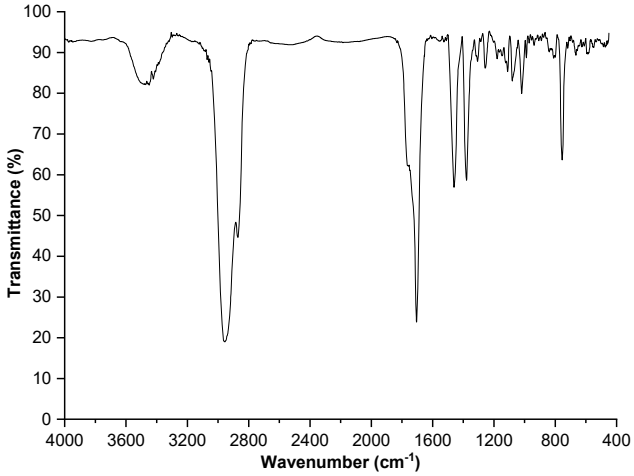

Fig S2. FTIR spectrum of (**1**)

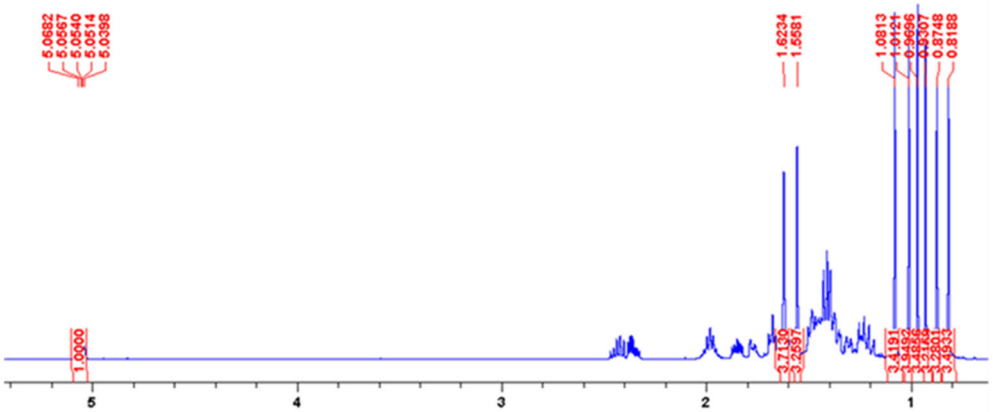

Fig S3. ^{1}H-NMR spectra of (**1**) (500 MHz in $CDCl_3$)

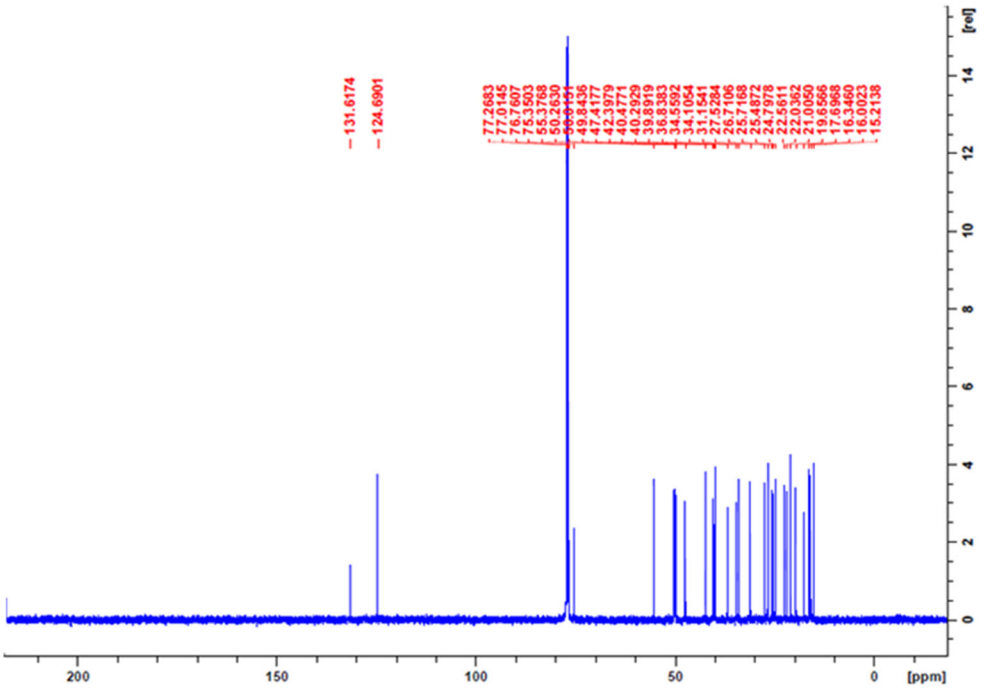

Fig S4. ^{13}C-NMR spectrum of (**1**) (125 MHz in $CDCl_3$)

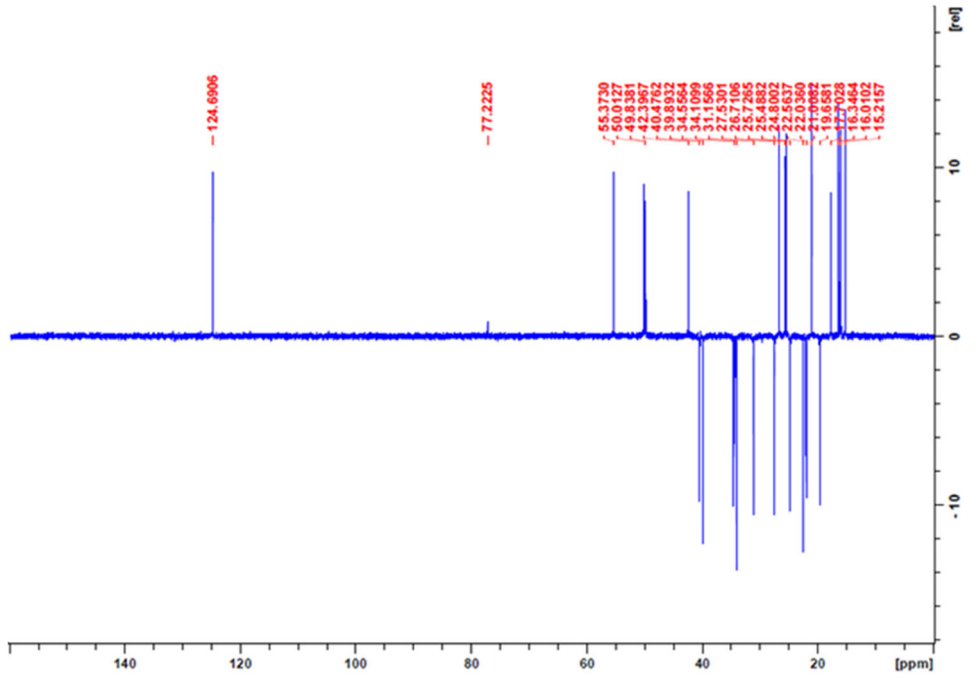

Fig S5. DEPT 135° spectrum of (**1**) (125 MHz in $CDCl_3$)

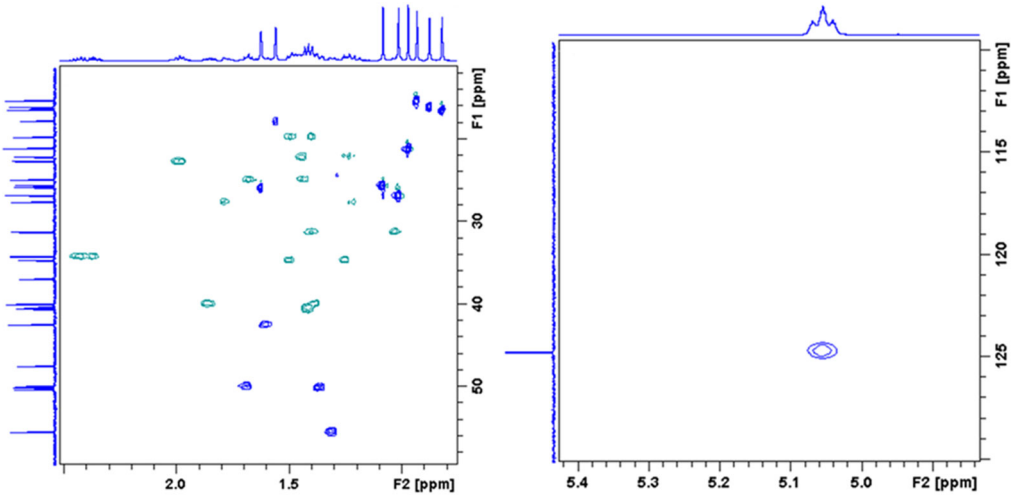

Fig S6. HSQC spectrum of (**1**)

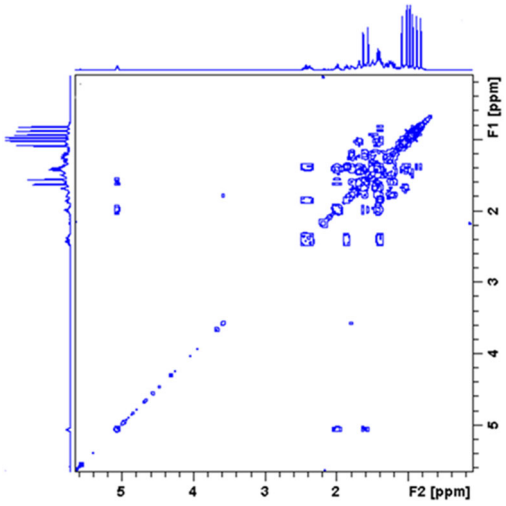

Fig S7. ^{1}H-^{1}H-COSY spectrum of (**1**)

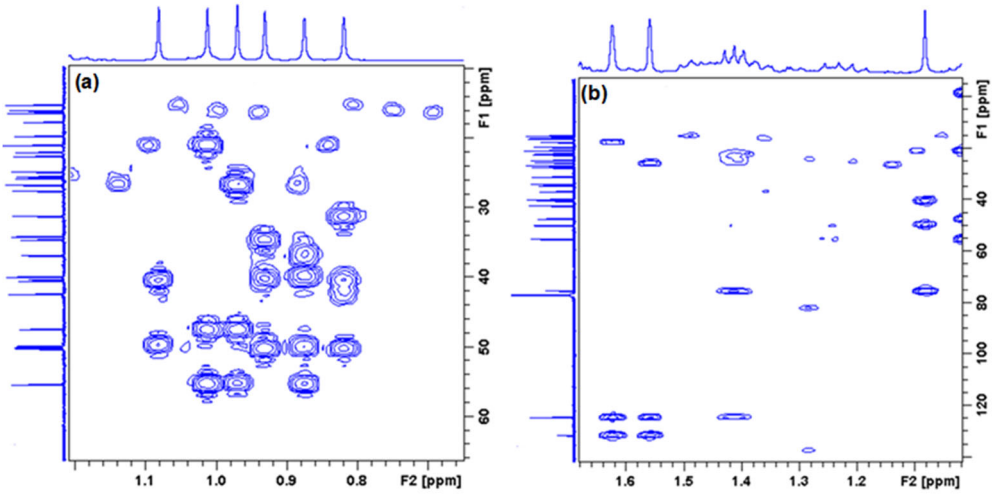

Fig S8. HMBC spectrum of (**1**)

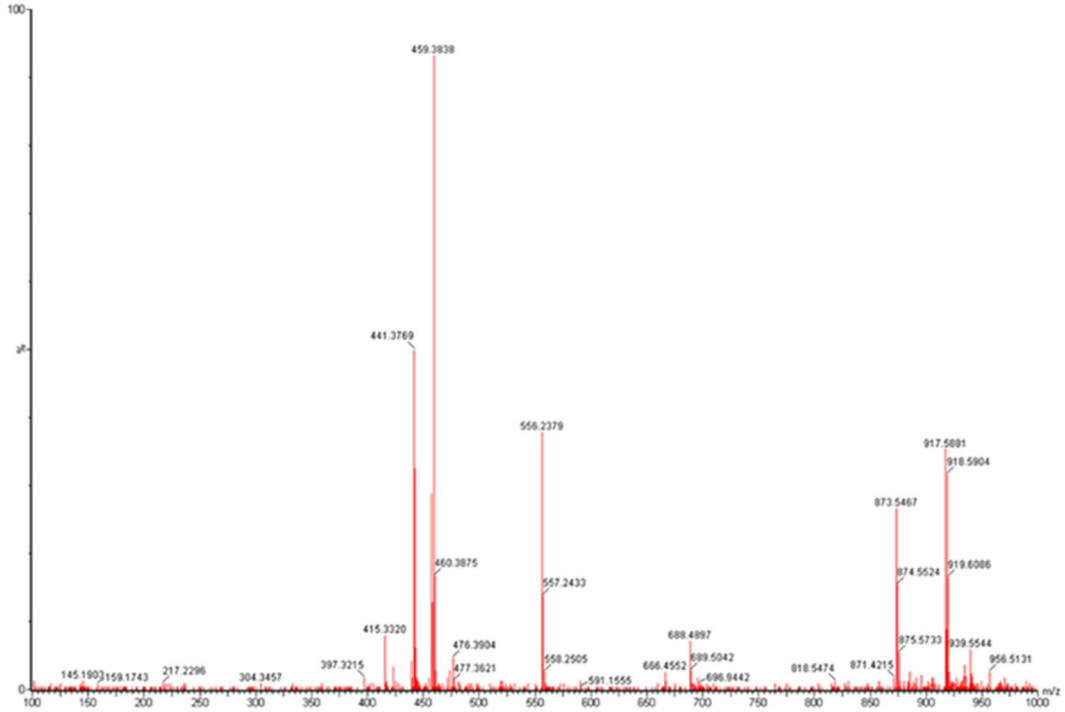

Fig S9. HR-TOFMS spectrum of (**2**)

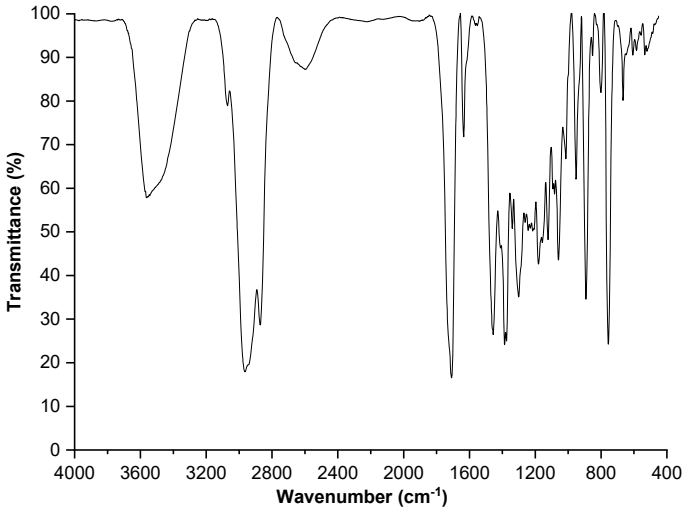

Fig S10. IR spectrum of (**2**)

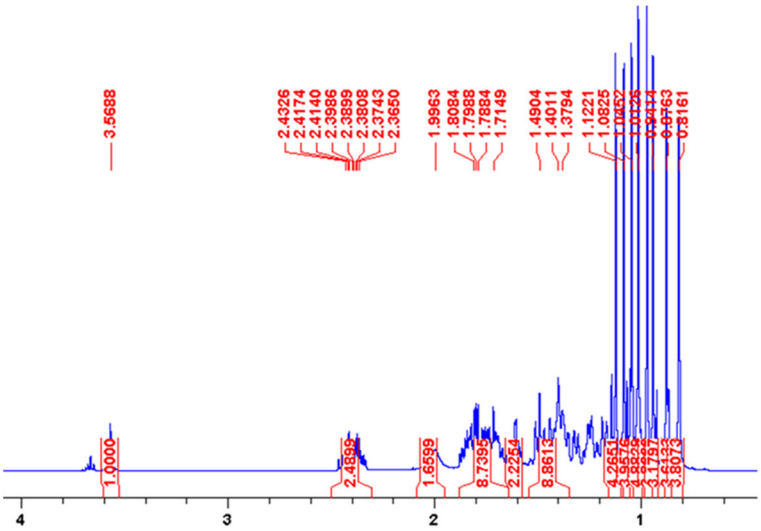

Fig S11. ^{1}H-NMR spectrum of (**2**) (500 MHz in $CDCl_3$)

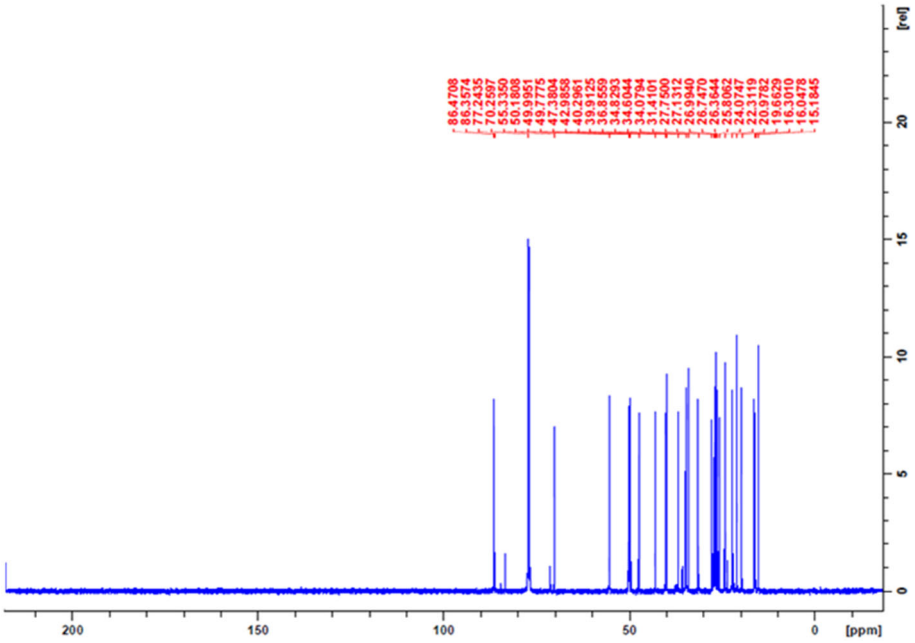

Fig S12. ^{13}C-NMR spectrum of (**2**) (125 MHz in $CDCl_3$)

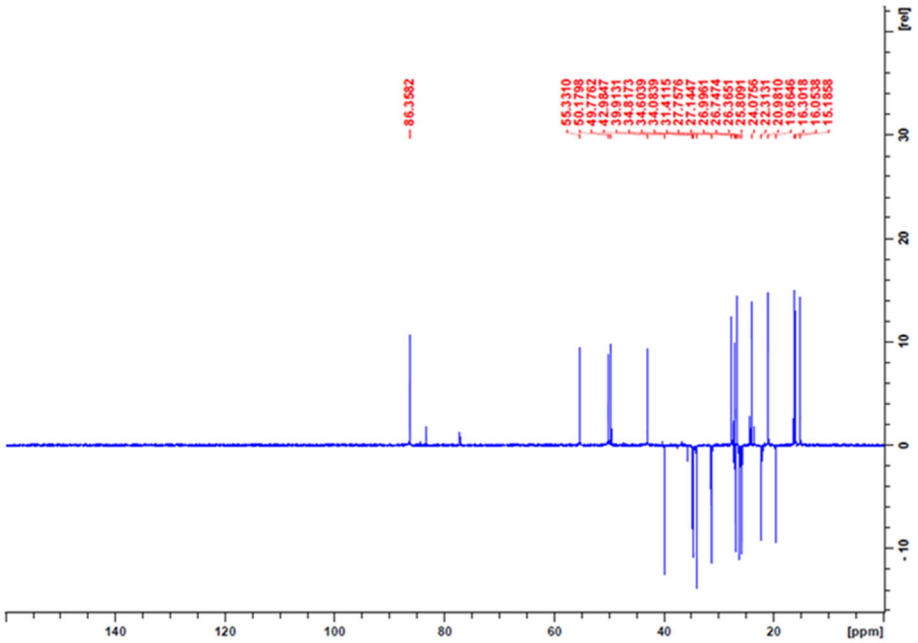

Fig S13. DEPT 135° spectrum of (**2**) (125 MHz in $CDCl_3$)

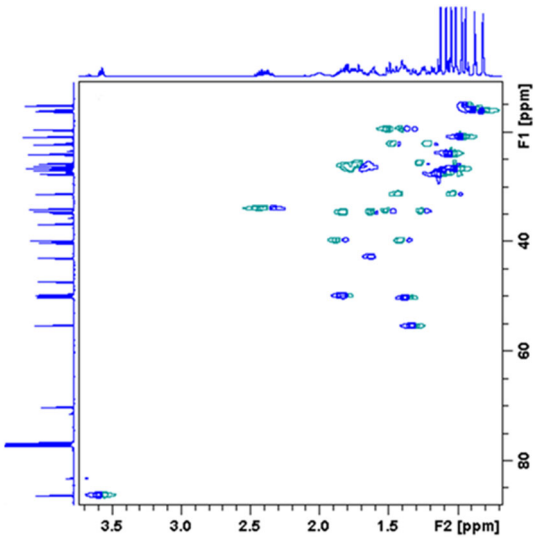

Fig S14. HSQC spectrum of (**2**)

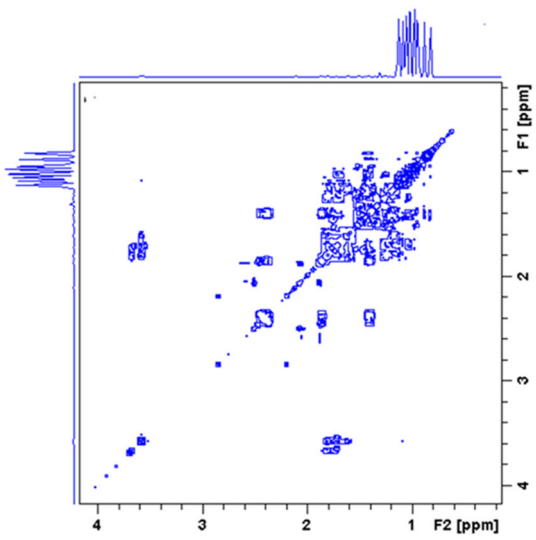

Fig S15. ^{1}H-^{1}H-COSY spectrum of (**2**)

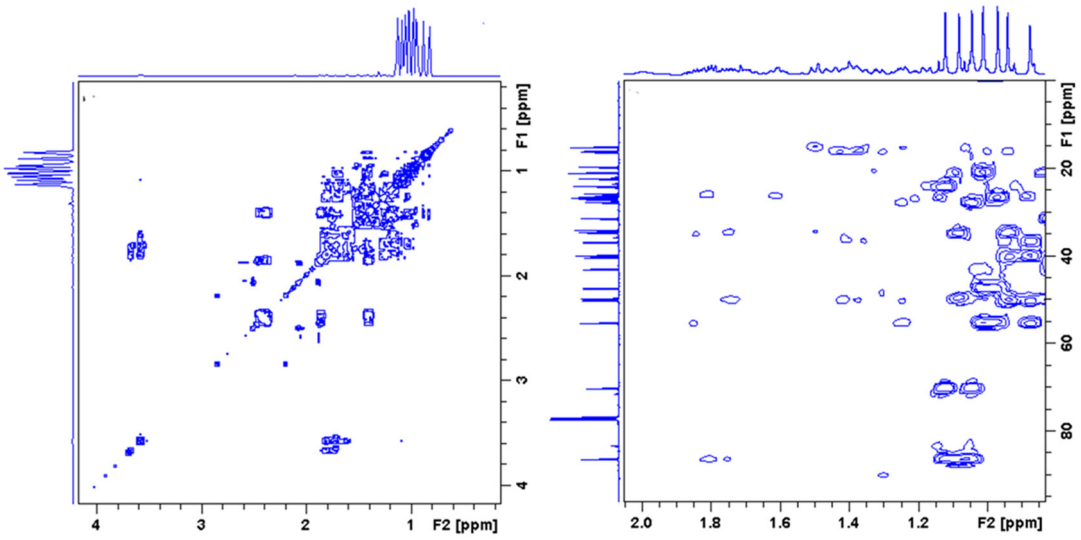

Fig S16. HMBC spectrum of (**2**)

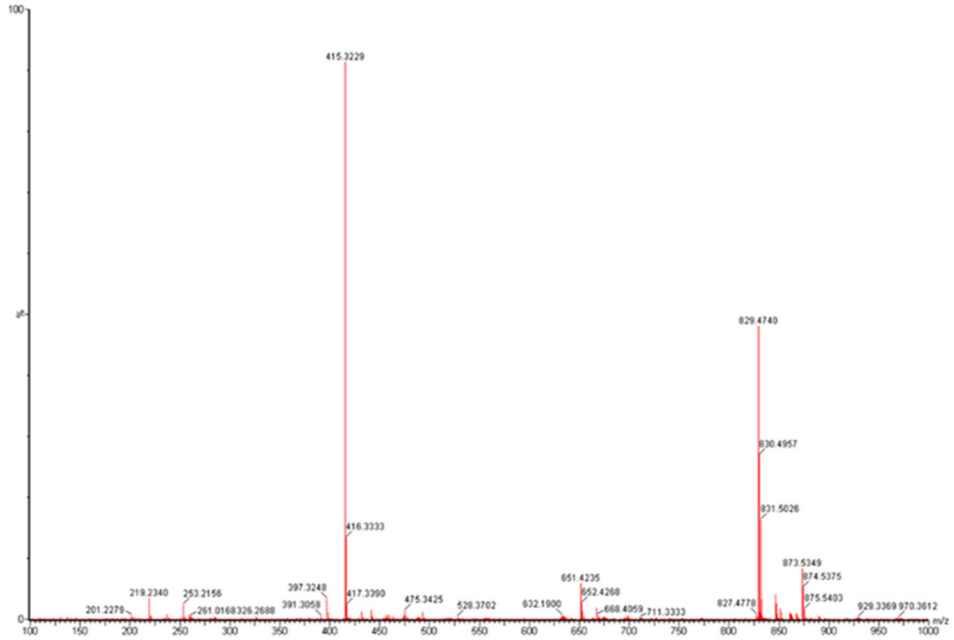

Fig S17. HR-TOFMS spectrum of (**3**)

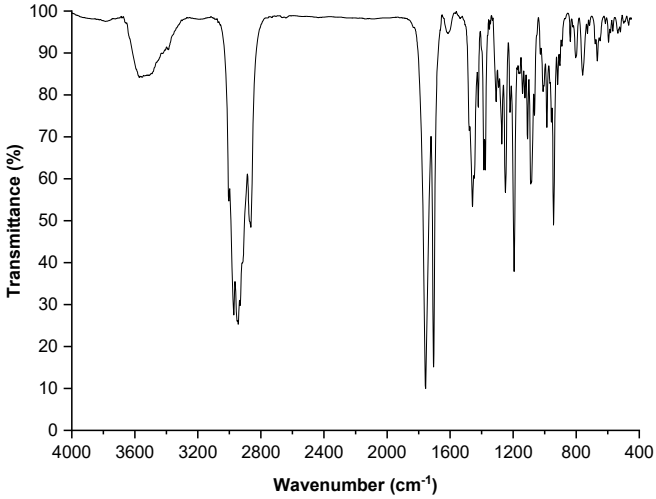

Fig S18. IR spectrum of (**3**)

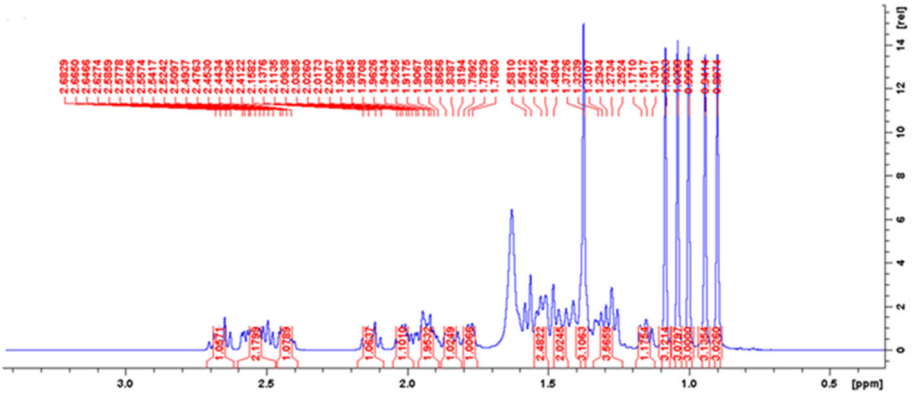

Fig S19. ^{1}H-NMR spectrum of (**3**) (500 MHz in $CDCl_3$)

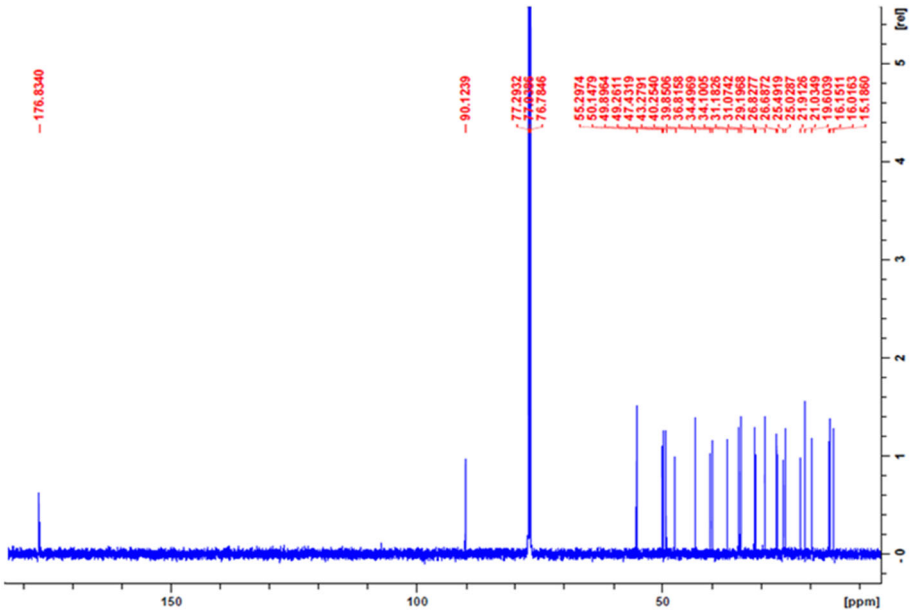

Fig S20. ^{13}C-NMR spectrum of (**3**) (125 MHz in $CDCl_3$

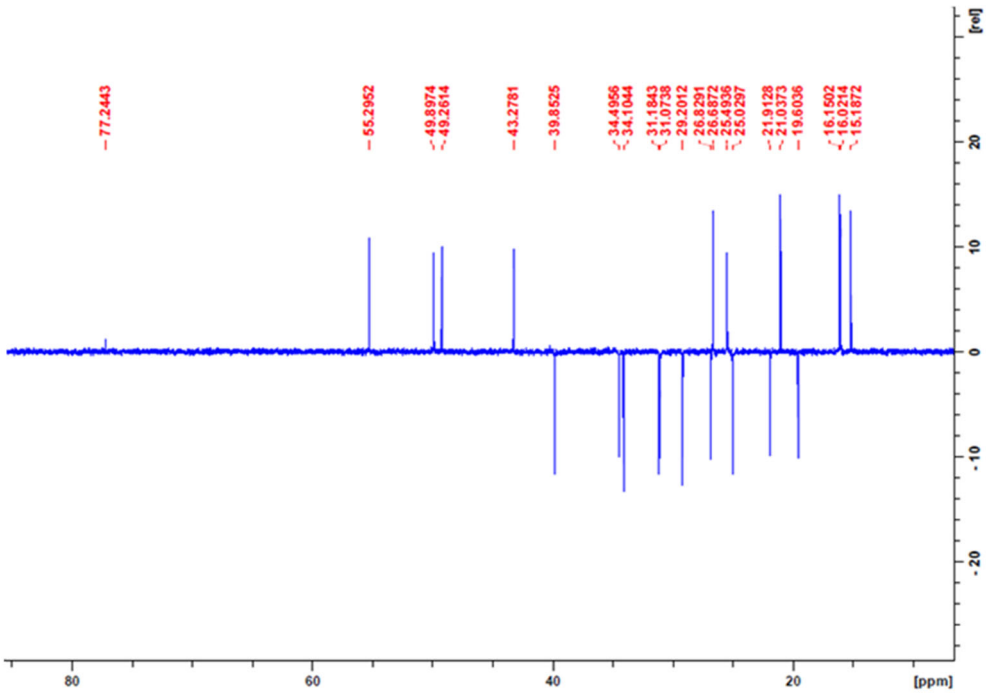

Fig S21. DEPT 135° spectrum of (**3**) (125 MHz in $CDCl_3$)

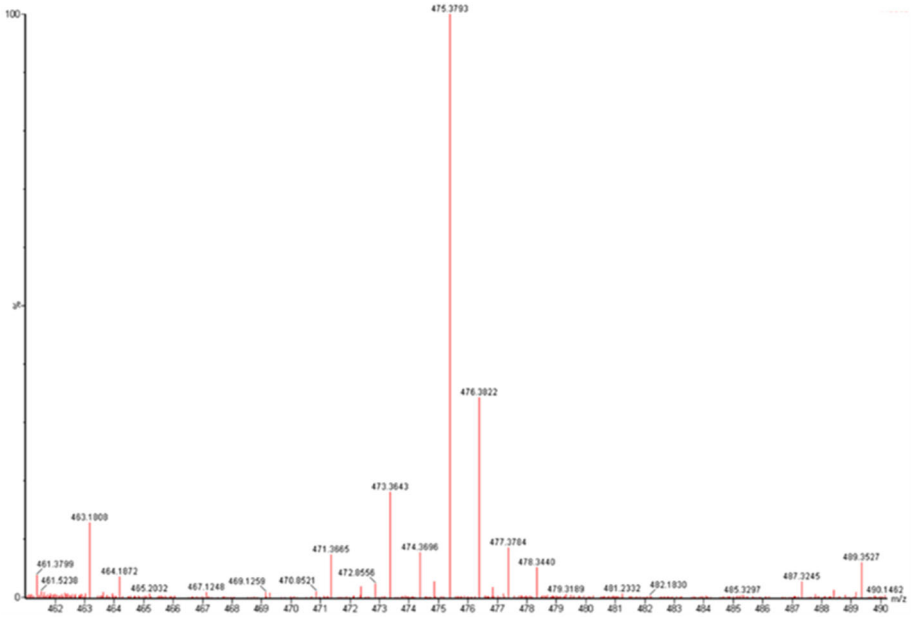

Fig S22. HR-TOFMS spectrum of (**4**)

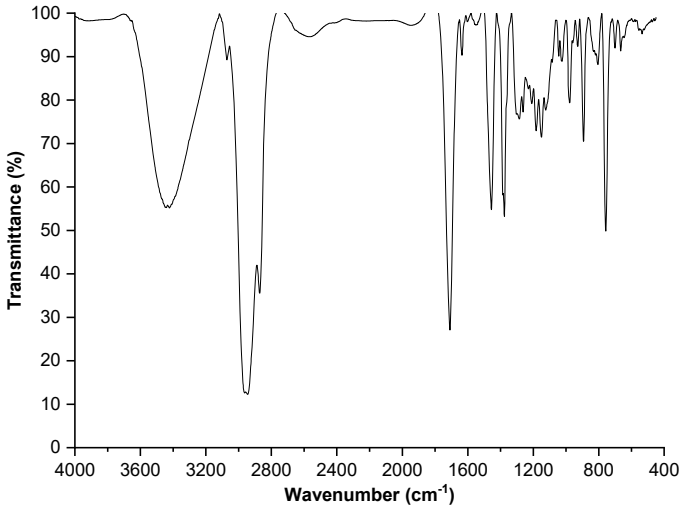

Fig S23. IR spectrum of (**4**)

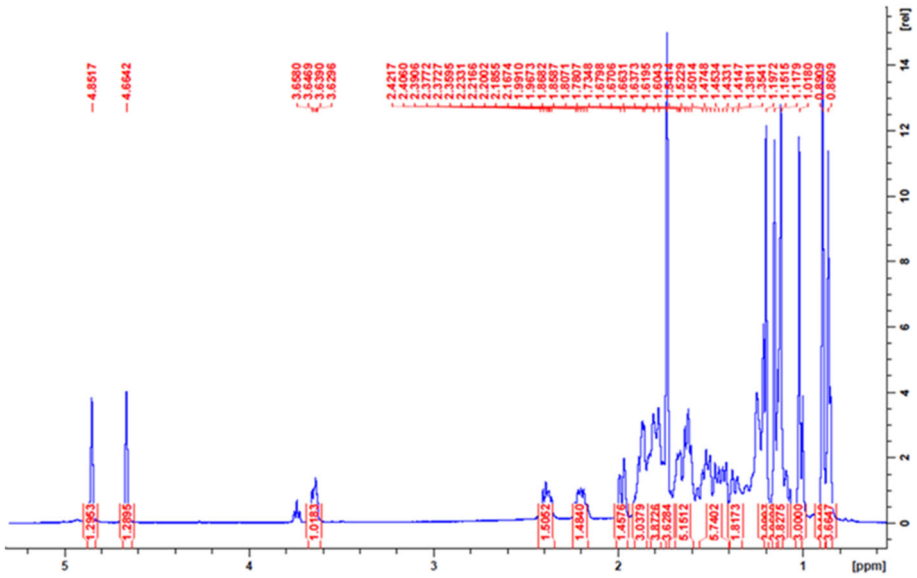

Fig S24. ^{1}H-NMR spectrum of (**4**) (500 MHz in $CDCl_3$)

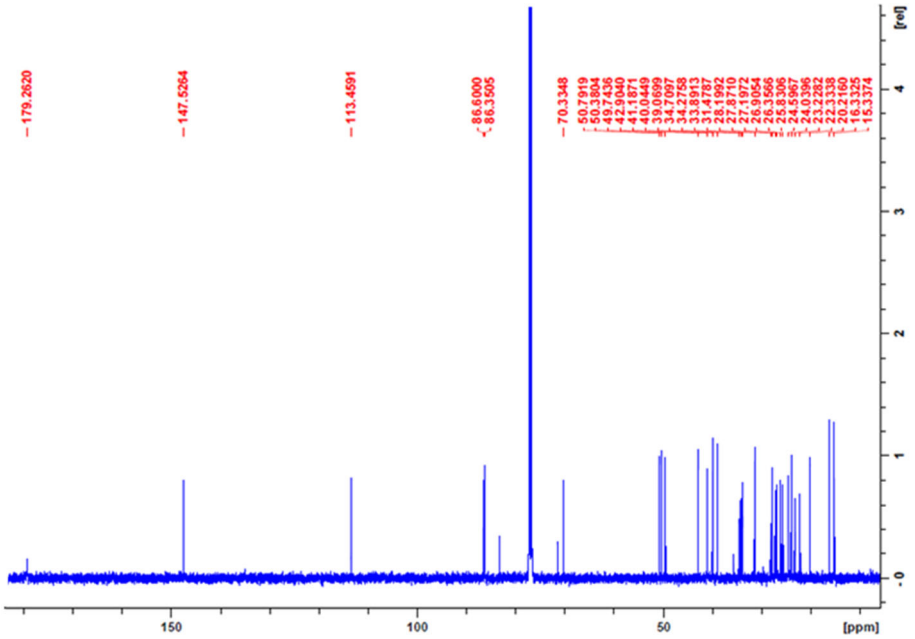

Fig S25. ^{13}C-NMR spectrum of (**4**) (125 MHz in $CDCl_3$)

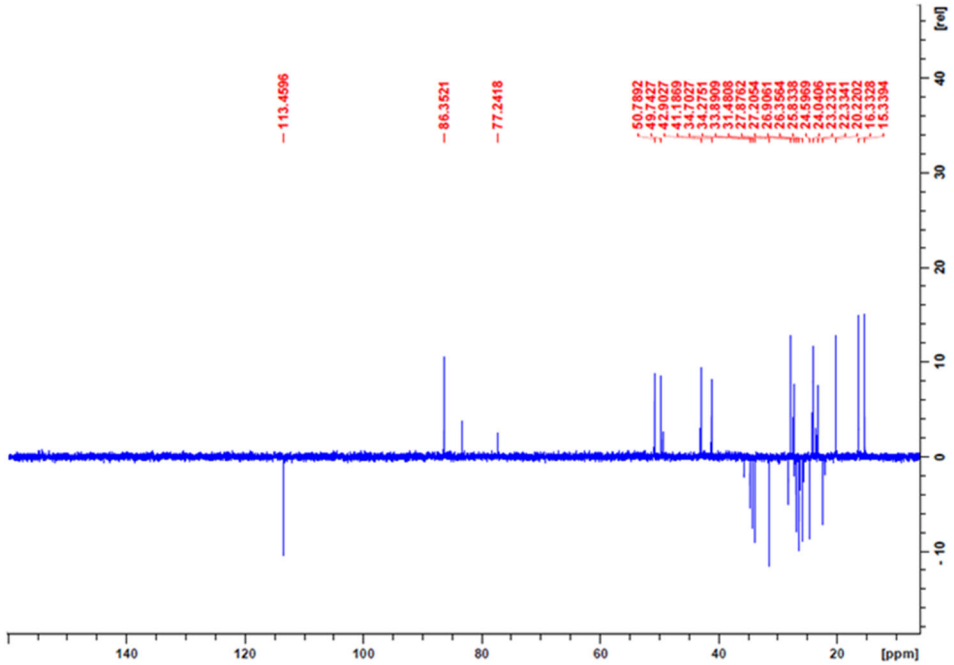

Fig S26. DEPT 135° spectrum of (**4**) (125 MHz in $CDCl_3$)

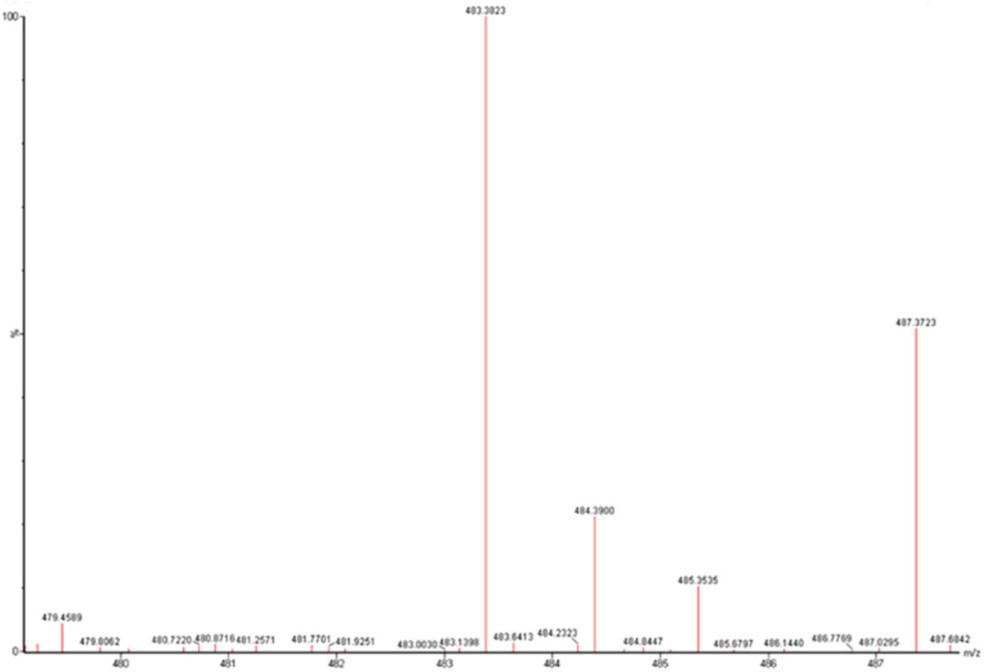

Fig S27. HR-TOFMS spectrum of (**5**)

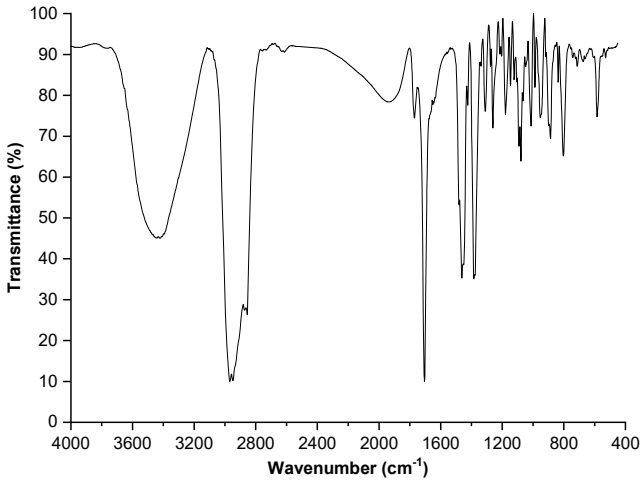

Fig S28. IR spectrum of (**5**)

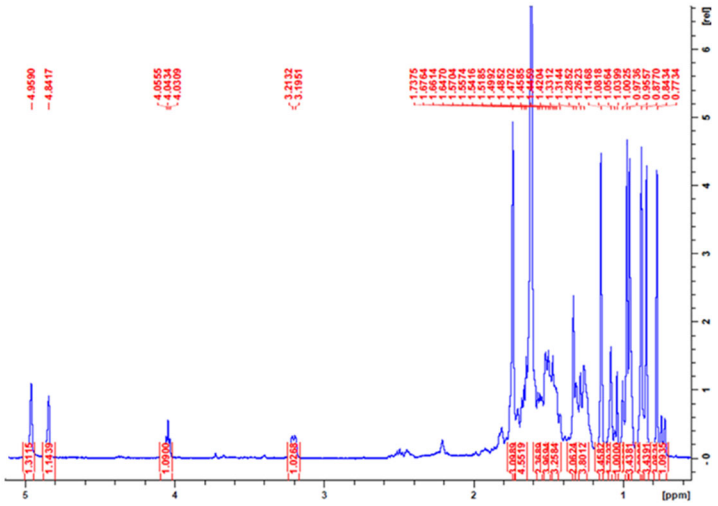

Fig S29. ^{1}H-NMR spectrum of (**5**) (500 MHz in $CDCl_3$)

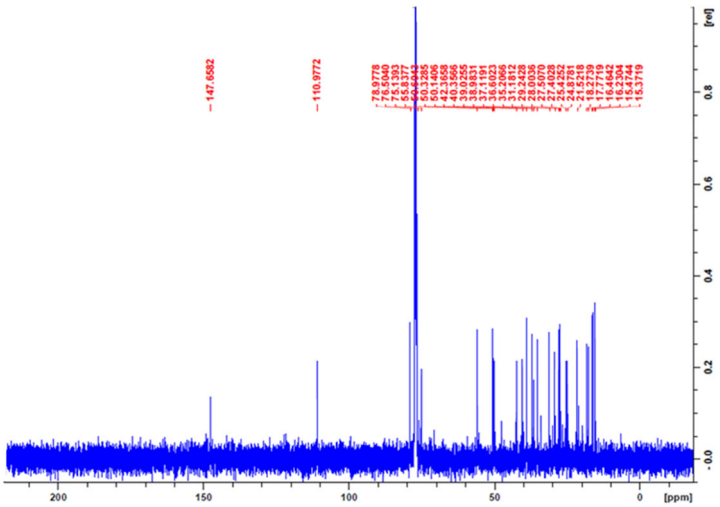

Fig S30. ^{13}C-NMR spectrum of (**5**) (125 MHz in $CDCl_3$)

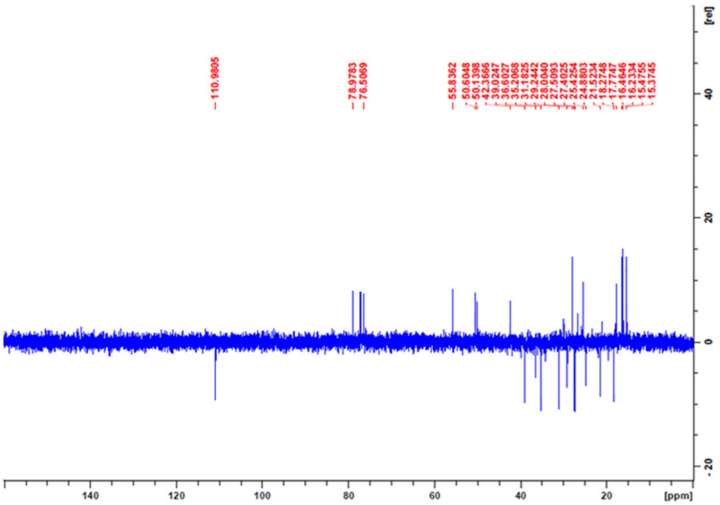

Fig S31. DEPT 135° spectrum of (**5**) (125 MHz in $CDCl_3$)